Construction and Building Materials 394 (2023) 132174

Contents lists available at ScienceDirect

Construction and Building Materials

journal homepage: www.elsevier.com/locate/conbuildmat

Behavior of large diameter carbon fiber anchors

Emrah Tasdemir [a,b,*], Rudolf Seracino [a], Mervyn J. Kowalsky [a], James Nau [a]

[a] North Carolina State University, Department of Civil, Construction, and Environmental Engineering, 27695-7908 Raleigh, NC, USA
[b] Bilecik Seyh Edebali University, Faculty of Engineering, Department of Civil Engineering, 11100 Bilecik, Türkiye

ARTICLE INFO

Keywords:
Carbon fiber anchors
Fan angle
Embedment depth
Large diameter
Strengthening
Repair
CFRP

ABSTRACT

The use of fiber anchors is becoming more commonplace as part of an FRP retrofit of concrete or masonry structures. Such anchors are typically small diameter (sometimes referred to as spike anchors) and are mainly used to delay, or possibly prevent, debonding of externally-bonded FRP laminates. However, capacity prediction models developed for small diameter fiber anchors may not be extended to large carbon fiber (CF) anchors, herein defined as an anchor with a diameter greater than 19 mm. In this study, commercially available 19, 25, and 32 mm diameter CF anchors were tested. First, the behavior of straight CF anchors embedded in concrete under direct tensile loading was examined to obtain the benchmark rupture capacity of the anchors. Embedment depths varied between 10 and 13 times the anchor hole diameter. Then, the behavior of fanned CF anchors under direct tensile load was investigated, considering fan angles of 37° and 57°. Finally, the effect of column bending on the behavior of CF anchors was studied by installing anchors on previously tested large-scale reinforced concrete column-footing subassemblies. It was found that the anchor diameter, anchor fan angle, anchor hole diameter, and embedment depth of the anchor dowel impact the behavior of large diameter CF anchors. Further, confinement of the anchor fan in column applications with hoop direction carbon fiber laminates was found to have a substantial impact on the failure mode of large diameter CF anchors. It was found that for 25 mm diameter CF anchors with a well confined anchor fan, approximately 50% of the straight anchor rupture capacity is possible with a 559 mm long anchor fan with fan angle of 37° and an embedment depth of the anchor dowel 10 times the anchor hole diameter.

1. Introduction

Existing reinforced concrete (RC) structures need to exhibit a specified level of performance to comply with requirements in seismic design guidelines. Under a seismic event, the strength and ductility of RC structural members may not be adequate to reach the desired performance. Carbon fiber-reinforced polymer (CFRP) systems are among the alternatives that can be used to enhance the performance of existing RC structures. In addition to the durability of CFRP systems when exposed to corrosive environments, the light-weight and high-strength and stiffness of CFRP systems are desirable in the seismic retrofit of existing RC structures. Further, in wet lay-up in-situ applications the flexibility of form to accommodate variable cross-sectional geometry is advantageous compared to other alternatives. The versatility of CFRP systems makes them an appealing option for a wide range of strengthening or repair applications. In some applications, continuity of load path also needs to be provided to transfer forces from externally bonded (EB) CFRP laminates at the ends of members to adjacent structural elements. Similarly, elements may act as an obstruction creating a discontinuity of longitudinal CFRP laminates. Carbon-fiber (CF) anchors, which are formed using a bundle of loose carbon fibers to provide a load path at the end of structural members or at the end of CFRP laminates are among the solutions that have recently been used. Common uses of fiber anchors in strengthening applications are shown in Fig. 1. Fig. 1a shows an example of shear strengthening T-beams with FRP U-wraps and fiber anchors. Koutas and Triantafillou [1] found that including fiber anchors in the shear strengthening system substantially increased the total shear capacity of the strengthened T-beams. Fig. 1b shows a typical flexural strengthening example of an RC beam with longitudinal EB FRP. Here fibers anchors are introduced to delay debonding failure of the FRP system to enhance the increase in flexural capacity. Eshwar et al. [2] conducted research on the flexural strengthening of beams with curved soffits. It was found that including fiber anchors as part of the strengthening system increased the flexural strength of the beam and prevented peeling of CFRP laminates. Fiber anchors are also used in the strengthening of RC frames with masonry infill walls as shown in Fig. 1c.

* Corresponding author.
E-mail address: emrah.tasdemir@bilecik.edu.tr (E. Tasdemir).

https://doi.org/10.1016/j.conbuildmat.2023.132174
Received 20 September 2022; Received in revised form 13 June 2023; Accepted 14 June 2023
Available online 21 June 2023

In this strengthening application, infill walls were integrated with an existing RC frame to develop a new lateral load resisting system [3]. CF anchors were implemented to prevent premature debonding of CFRP laminates, and create a load path between the end of the CFRP laminate and the RC members. The detailed discussion regarding load transfer mechanism can be found in [3]. The developed strengthening scheme was shown to be effective in increasing the lateral load capacity of the RC frame. As shown in Fig. 1d, fiber anchors can be used in the flexural strengthening of RC shear walls where the ends of the vertical CFRP laminates can be anchored providing continuity of load path through the integral RC floor system. Lau and Woods [4] conducted research on shear walls strengthened with vertical CFRP laminates that were anchored to the adjacent concrete members with glass fiber anchors. It was revealed that anchoring the end of the vertical CFRP laminate increases the flexural capacity of the shear wall. El-Sokkary et al. [5] studied the seismic behavior of CFRP strengthened RC walls. The walls were strengthened with vertical CFRP laminates that were bonded to the left and the right corners of the wall, and the ends of vertical CFRP laminates were anchored with CF anchors that were produced from CFRP laminates. The flexural behavior of the wall was found to be improved. Flexural strengthening of RC columns with longitudinal CFRP is a common application where CF anchors are used to anchor the end of longitudinal laminates across the footing interface, as shown in Fig. 1e, so that the tension force in the CFRP may be developed at the maximum moment region. Vrettos et al. [6] studied the impact of the number and the volume of CF anchors on the flexural capacity of RC columns. It was concluded that the flexural capacity of columns can be increased by the use of CF anchors. But design details and recommendations, such as fan angle of the CF anchor, were not provided. Rutledge et al. [7] utilized CF anchors in the repair of seismically damaged RC columns. Twelve 30 mm diameter CF anchors were used to provide the force-transfer mechanism to resist the large tensile forces at the column-footing interface. The anchors strengthened the failed (plastic hinge) section of the column such that subsequent damage occurred in a previously

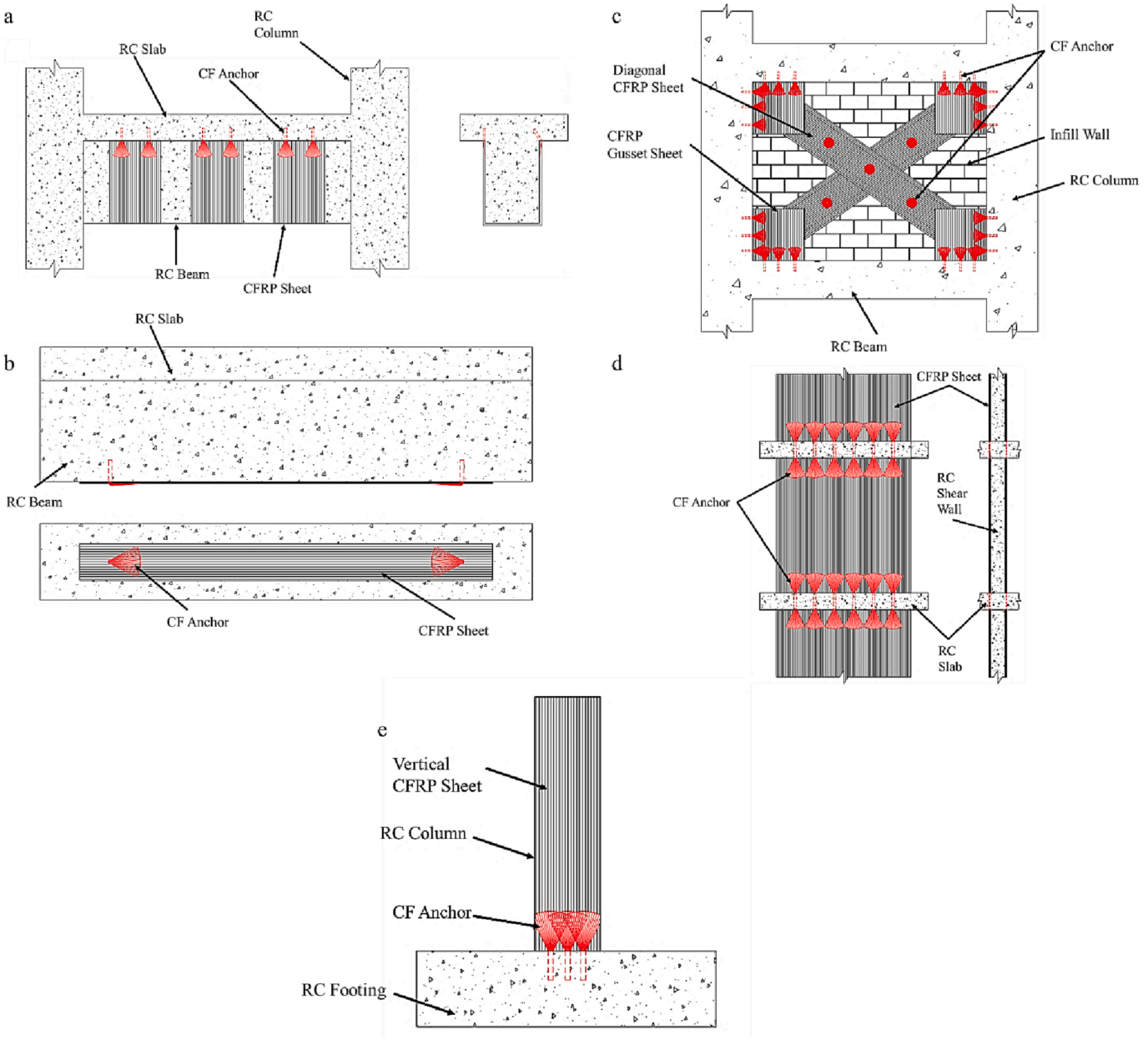

Fig. 1. CF Anchor Applications a) Shear Strengthening of T beam b) Flexural Strengthening of Beam c) Integrating Infill Wall with RC Frame d) Flexural Strengthening of RC Wall e) Flexural Strengthening of RC Column.

undamaged portion of the column. However, a detailed understanding of the design and behavior of the 30 mm diameter CF anchors was not achieved as part of that research project. del Rey Castillo et al. [8] presented research where straight CF anchors were used to increase the moment capacity of square RC columns. In the study, five square RC columns were repaired with varying number of CF anchors that had fiber area of 84 mm^2 (nominal diameter of 10 mm), 112 mm^2 (nominal diameter of 12 mm), and 168 mm^2 (nominal diameter of 15 mm). Anchor fan details were not reported. The study showed that CF anchors increase the lateral force capacity of square RC columns and tension–compression cycles did not impact the contribution of CF anchors to the lateral force capacity.

A typical application of a large diameter CF anchor is shown in Fig. 2, where the anchor is providing continuity of load path across an interface. Fig. 2a defines the primary parts of a large diameter CF anchor, and Fig. 2b shows the primary geometric parameters affecting the tensile strength. In this application, the anchor dowel fibers are installed into a drilled hole filled with epoxy resin while the anchor fan fibers are splayed over a CFRP laminate that is bonded to an existing RC member. The location where the anchor fibers transition from the dowel to the fan is referred to as the key portion.

There have been many research studies that focus on different parts of CF anchors defined in Fig. 2. Kim and Smith [9], Ozdemir and Akyuz [10], and Ozbakkaloglu and Saatcioglu [11] focused on the parameters affecting the pull out capacity of fiber anchors. A pull out capacity prediction model was developed by Kim and Smith [9]. It should be noted that the developed model is restricted to the anchor diameters used in the derivation. For anchor diameters larger than 19 mm, the accuracy of the model is not known with sufficient certainty. Kobayashi et al. [12] carried out an experimental program to investigate the influence of fan angle on the capacity of CF anchors. The fan angle was varied from 47° to 120°. The fan angle was found to be a factor affecting the tensile capacity of the anchors. del Rey Castillo et al. [13] conducted an experimental study to evaluate the effect of fan angle ranging from 30° to 120° on the behavior of CF anchors. It was found that for the same diameter anchor, an increase in fan angle yields lower anchor capacity. Also, larger diameter CF anchors were found to be less efficient than CF anchors with a smaller diameter. A capacity prediction model that considers fan angle and anchor diameter was developed. Although a large number of CF anchor tests are published in the open literature, a unified design approach has yet to be established due to the large variation in the parameters affecting the design and behavior of fiber anchors, such as: anchor diameter; fan angle; fan length and fan width; embedment depth of anchor dowel; material properties of dry fibers, epoxy and concrete; and the quality of anchor installation. The lack of design guidelines limits the extensive utilization of fiber anchors in EB strengthening or repair applications [14], although numerous research studies have shown the effectiveness of fiber anchors in postponing or preventing debonding of FRP systems. ACI 440.2R [15] allows the use of fiber anchors in EB applications on the condition that the effectiveness of the anchorage system is demonstrated by representative tests. However, standardized testing protocols are not suggested [16], nor available, further hindering the widespread use of fiber anchors in EB FRP retrofit applications.

Seismic damage in RC bridge columns, which are designed according to modern seismic guidelines, occurs at plastic hinge regions designed to be at either end of columns. Failure typically occurs due to buckling and fracture of reinforcing bars subjected to large plastic strains. Repair of such severely damaged bridge columns requires a substantial intervention if the original column behavior is to be restored. Large diameter CF anchors, as part of an FRP repair, was shown to be an effective way to restore the original column behavior following the formation of a plastic hinge [7]. This was accomplished by strengthening the damaged region such that damage from a subsequent seismic event would occur elsewhere in the column. The technique is referred to as “plastic hinge relocation”. Unfortunately, the absence of design details for such large diameter CF anchors prevents the generic application of robust repair solutions. Therefore, there is a need to examine the behavior of large diameter CF anchors designed to transfer tensile forces across column-to-footing interfaces to restore the response of seismically damaged RC columns.

The research presented herein focuses on the tensile behavior of commercially available large diameter (≥19 mm) CF anchors. An experimental program was developed to understand the theoretical rupture capacity of CF anchors by pulling on straight anchors embedded in concrete blocks. Anchor diameters of 19 mm, 25 mm, and 32 mm were tested. Results of the tests are presented in terms of efficiency to identify the impact of each parameter. The effect of fan angle on the capacity of the anchor was also investigated on 25 mm diameter anchors with fan angles ranging from 37° to 57°. The significance of fan angle on the capacity of CF anchors is discussed by presenting the efficiency distribution of all 25 mm diameter anchors tested, including straight anchors. In addition, the behavior of 25 mm diameter CF anchors under column bending was tested to determine the effect of bending on the parameters affecting anchor capacity obtained from direct tension pull out tests. A design procedure to provide sufficient bond between the anchor fan and the concrete substrate is suggested. The data obtained from the research presented herein is part of a larger research study that aims to develop a repair methodology for seismically damaged RC bridge columns.

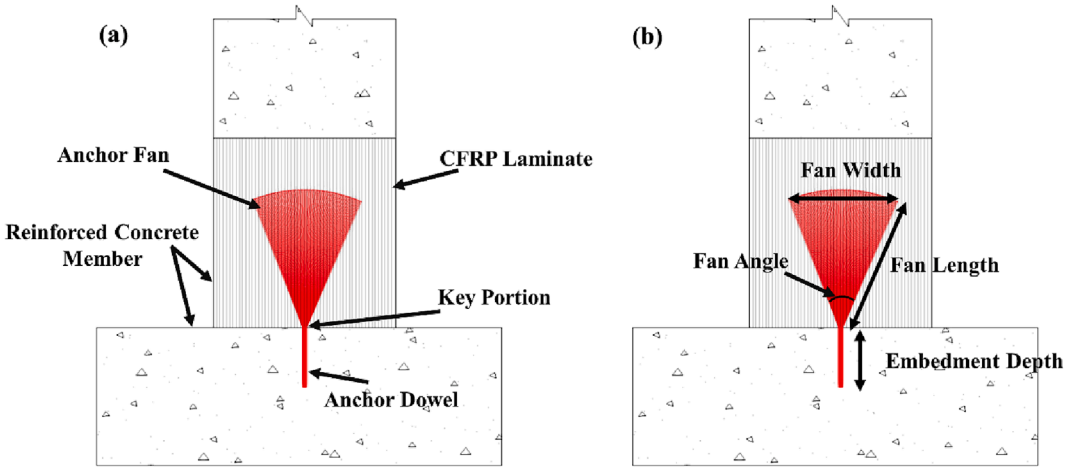

Fig. 2. CF Anchor: a) Parts b) Geometric Parameters.

2. Experimental program

The goal of the research study presented herein was to better understand the tensile behavior of large diameter CF anchors and utilize the same anchors in the repair of large-scale RC bridge columns damaged under simulated earthquake loading. To achieve this goal three sets of experiments were conducted with the aim of developing a comprehensive understanding of the behavior of large diameter CF anchors. The first set of anchor tests was designed to study the tensile capacity of straight CF anchors with various dowel diameters and embedment depths. The second set of anchor tests evaluated the impact of fan angle on the tension capacity of large diameter CF anchors. Finally, the third set of tests was conducted on large-scale circular RC columns where the anchor fan was splayed on the column concrete substrate and the dowel embedded into the footing. The purpose of the third set of tests was to investigate the effect of column bending on the tensile capacity of the anchor, and the bond between the column concrete substrate and the anchor fan.

2.1. Material properties

Two different CF anchors, procured from two manufacturers, were used in this research program. The CF anchors used in the straight anchor tests had tensile strength, tensile modulus, and elongation at rupture of 986 MPa, 96 GPa, and 1.20 %, respectively, according to laminate properties provided by the manufacturer. The CF anchors used in the fanned anchor and column tests had tensile strength, tensile modulus, and elongation at rupture of 1447 MPa, 99 GPa, and 1.46%, respectively, according to laminate properties provided by the manufacturer. The CFRP laminate properties provided by the manufacturer used in the fanned anchor and column tests were assumed to be similar to the CF anchors used in the straight anchors test, in order to examine the impact of anchor fan on the capacity of CF anchors. The concrete blocks used in the straight and fanned anchor tests were cast more than a year before the anchor tests were undertaken and had an average compressive strength of 49.6 MPa as determined by tests on standard 100 mm diameter by 200 mm concrete cylinders at the time of testing. Thus, concrete compressive strength was not included as a parameter in the experimental program.

2.2. Direct tension tests

2.2.1. Test setup for direct tension test

Several fiber anchor test methods have been developed, but to-date no standardized test method has been proposed [16]. A challenge of developing a standardized test method is that fiber anchors may be used

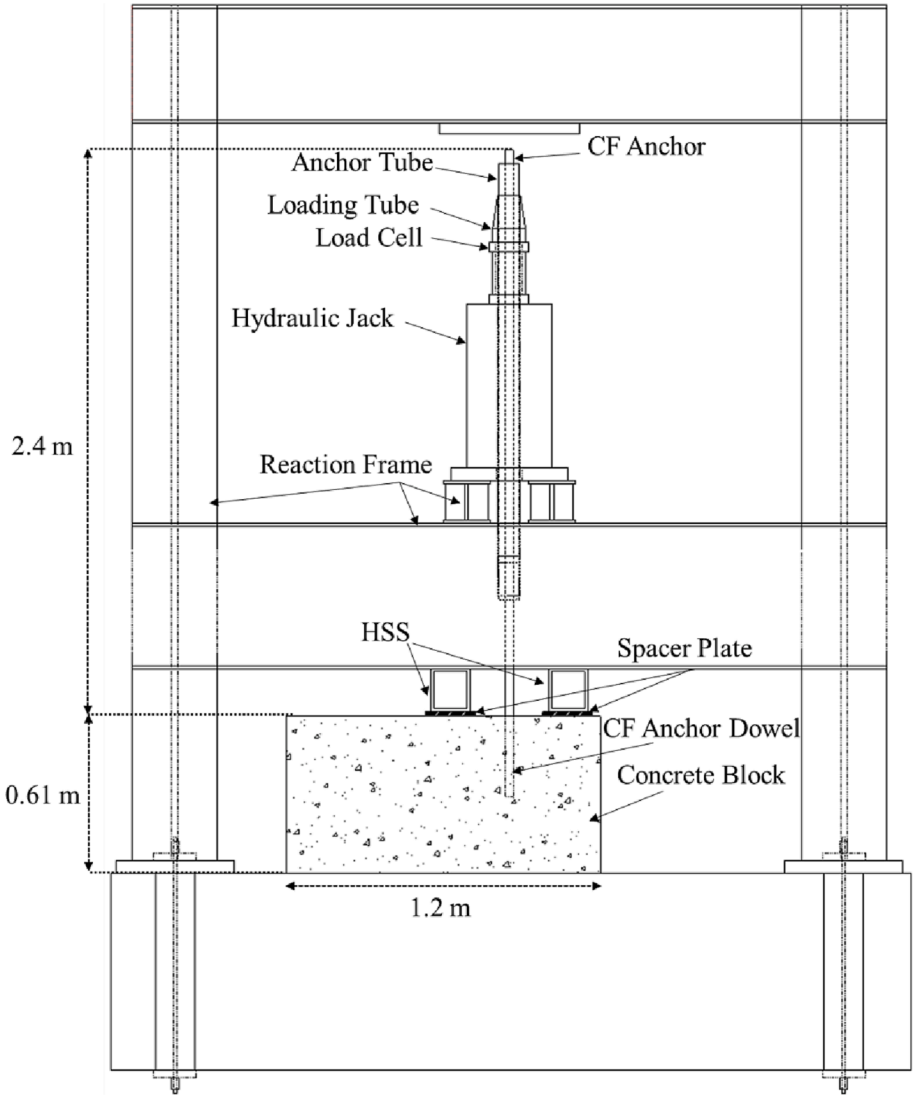

Fig. 3. General View of Test Setup for Straight Anchor Tests.

in several different configuration. Consequently, ACI 440.2R [15] recommends that the capacity of fiber anchors should be determined by demonstrative tests simulating the field application. ASTM D7205 [17] was developed for solid circular glass FRP (GFRP) bars with diameter less than 32 mm, and for CFRP bars with a diameter of 9.5 mm. ASTM D7205 [17] recommends anchoring the FRP bar into steel pipes at its ends where the annular ring is filled with a resin or grout. In this manner, the steel pipes can be gripped to pull the FRP bar in direct tension using a universal testing machine to determine the tensile rupture capacity. As the tension capacity of the large diameter CF anchors considered in this study is expected to be greater than what would be achieved by the GFRP bars covered by ASTM D7205 [17], the recommended testing details may not be directly transferable. Moreover, the testing method of ASTM D7205 [17] does not represent the field application where the circular anchor dowel is embedded into the concrete. To represent the embedment of large diameter CF anchor dowels in a field application the test setup shown in Fig. 3 was developed. The setup consisted of three main parts, including: a 1.2 m × 1.2 m × 0.61 m concrete block; a reaction frame; and the loading system comprised of a loading tube, anchor tube, load cell and hydraulic jack. A detailed schematic of the loading system is shown in Fig. 4. With a slight modification, the test setup was also used to test the CF anchor fan, as shown in Fig. 5.

A 2700 kN hollow hydraulic jack, which had a 100 mm diameter hole, was utilized. The hydraulic jack was placed on a 51 mm thick 457 mm square steel plate that was supported on two structural steel beams. A 100 mm diameter hole was drilled through the center of the 457 mm square steel plate to allow the loading tube to pass through. The two structural steel beams were connected to the reaction frame to transfer force from the hydraulic jack to the CF anchor through the loading tube.

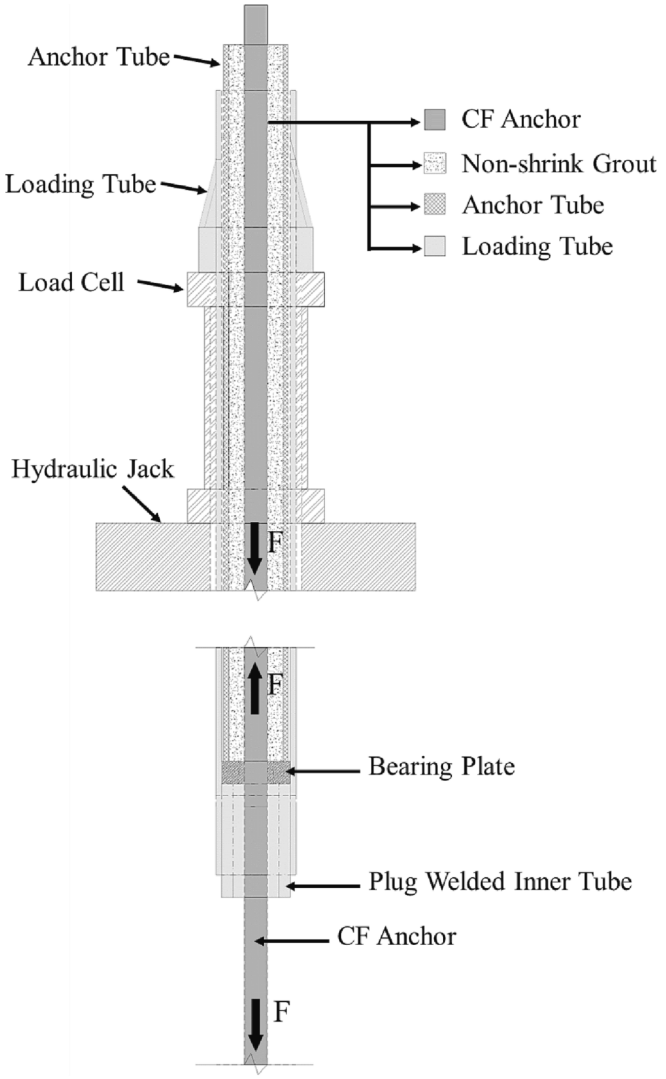

Fig. 4. Loading System Details for Straight and Fanned Anchors.

To transfer load from the hydraulic jack to the CF anchor, a loading tube was designed and constructed. A 1.5 m long steel tube, which had a 90 mm outside diameter (OD), was used to construct the loading tube. A 50 mm thick steel plate with a 90 mm hole was welded 152 mm below the top of the loading tube. In addition, four gusset plates were welded to the steel plate and loading tube with fillet welds to avoid bending of the steel plate. With this configuration of the plate, the loading tube can be placed on top of the load cell. As a result, the force in the hydraulic jack can be transferred to the loading tube. To create a force transfer mechanism between the loading tube and the anchor tube, a 127 mm long steel tube was placed and plug welded to the bottom inner side of the loading tube. The outside diameter and the wall thickness of the tube were 76 mm and 13 mm, respectively. With the help of the inner tube, the load was transferred to the anchor tube through the bearing plate which was positioned between the anchor tube and the inner steel tube. A bond mechanism was developed by gripping the top (free end) of the CF anchor through the approach recommended in ASTM D7205 [17]. The free end of the anchor was pulled through the anchor tube that had an outside diameter and wall thickness of 76 mm and 6 mm, respectively. The anchor tube was 1.5 m long to have sufficient bond length and prevent slip of the CF anchor. The annular ring was filled with a commercially available high-strength non-shrink grout.

In order to restrain the concrete block during loading of the CF anchor, hollow structural sections (HSS) were placed between the concrete block and the reaction frame, as shown in Fig. 3. Four 200 mm × 200 mm × 50 mm spacer plates were located underneath the HSS to keep the HSS above the concrete block and avoid compressive stress transfer near the anchor hole area in the concrete block. Later, for anchor fan tests the steel spacer plates were removed as there was no need to prevent compression stress transfer. With this configuration, a self-reacting mechanism was produced so that no tie bars were required to tie concrete blocks to the strong floor. CF anchors tested on the same concrete block were located at least 610 mm away from previously tested anchors and 305 mm away from the edge of the block, so that the same block may be used for multiple tests. In addition, the vertical dimension of the HSS and spacer plates enabled the placement of LED markers as part of a non-contact 3D displacement measurement device on the exposed length of the CF anchor.

2.3. Instrumentation

2.3.1. Pull test

The load cell was manufactured by welding two 38 mm thick plates with a concentrically located 100 mm diameter hole to the top and bottom of a 140 mm diameter hollow steel tube, which was 152 mm long. Later, four strain gauges were placed around the steel tube to create a Wheatstone bridge to read the resistance that was used to determine the corresponding force. The manufactured load cell was calibrated using a universal testing machine. To measure tensile force on the CF anchor, the load cell was placed between the loading tube and the hydraulic jack.

In order to measure the strain developed in the CF anchor during testing, a non-contact optical measuring system (OPTOTRAK) was used. The system includes a sensor, LED markers, and a data acquisition system to record the real-time 3D location of the LED markers attached to the surface of the exposed length of the CF anchor. In this test program, three LED markers were placed on the CF anchor at a nominally 50 mm gauge length, as shown in Fig. 6. The average strain over the gauge length is calculated using the recorded 3D location of the LED markers.

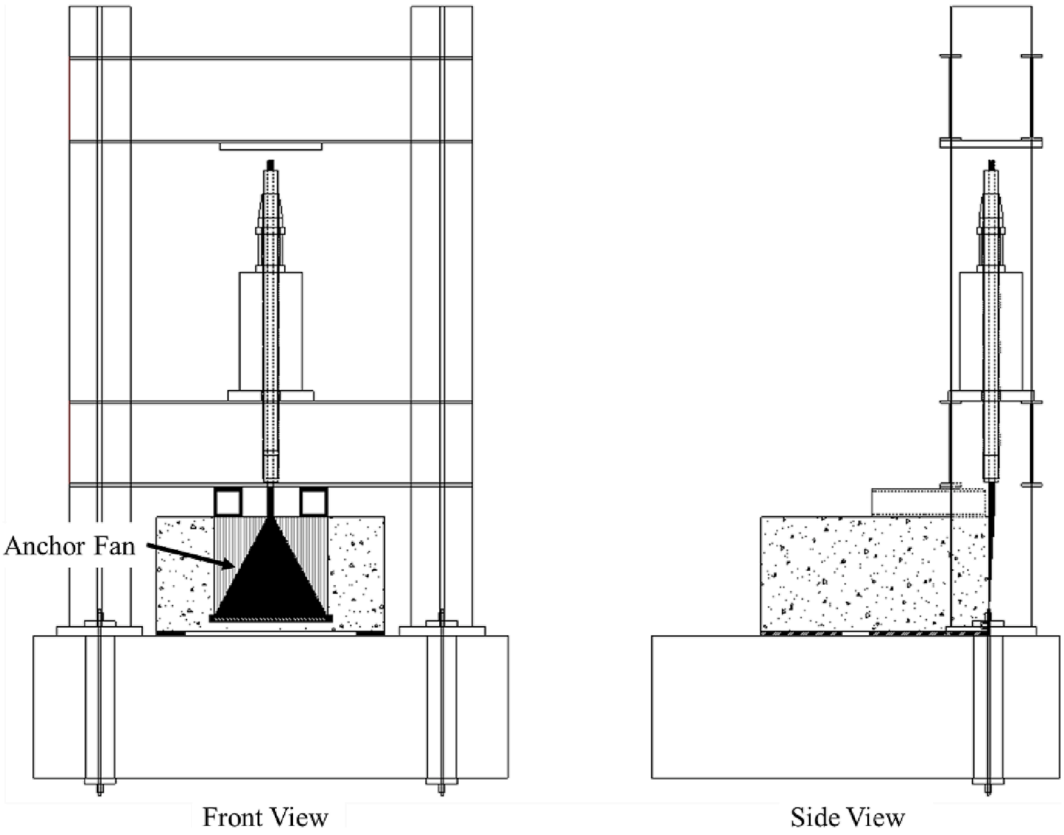

Fig. 5. General View of Test Setup for Fanned Anchor Tests.

2.4. Preparation of specimens

During the test program it was realized that quality control of the anchor installation procedure has a greater effect on the behavior and capacity of the CF anchors than originally anticipated. Therefore, the installation procedure was modified during the test program. Further, the outcomes of the different installation procedures were used to quantify the variability of the CF anchor capacity.

2.4.1. Pull test specimens

The CF anchors were prepared following the manufacturer's recommendation for field application where the entire length of the anchor is saturated with provided two-component epoxy. The anchor is then inserted into a pre-drilled hole filled with epoxy via the loop end using a smooth steel bar. A schematic of the installation procedure is shown in Fig. 7. For the first four tests, the 2.7 m long anchors used in this test series were saturated and inserted in the pre-drilled holes. However, given the high variability of the recorded data due to the variable quality of the manufacture and installation of the anchor, the manufacturing method was slightly modified for the subsequent tests. A detailed discussion of the results is presented later. In an attempt to improve alignment of the carbon fibers and reduce the initial variability observed, the 2.7 m long CF anchors were pulled through PVC pipes forming a nearly circular cross-section. This method showed improvement but still misalignment of the fibers was identified as the main reason that full anchor capacity was not achieved. Hence, the preparation method was further modified to improve fiber alignment and reduce flaws caused by the preparation procedure. In the revised preparation method, the carbon fibers were saturated as shown in Fig. 8a, pulled through 1.2 m long PVC pipes, with an inner diameter equal to that of the anchor diameter, and hung vertically. Then, the fibers were aligned by hand as shown in Fig. 8b. Once the anchor cured, the bottom end was cut to obtain a flat surface, eliminating the misaligned fibers, as shown in Fig. 8c. This was done to ensure that the anchor remains straight after installing into the predrilled anchor hole. Finally, the cured CF anchor was inserted into a predrilled hole that was filled with the same two-component epoxy used in the saturation process, as shown in Fig. 8d. Once the hydraulic jack, load cell, loading tube and anchor tube were in place, a high-strength non-shrink grout was poured into the annular ring to create the bond between the anchor and anchor tube. The anchors were tested seven days after pouring the high-strength non-shrink grout.

2.4.2. Fan test specimen

The previous test setup was slightly modified to enable the anchor fibers to be splayed on the face of the concrete block to observe the impact of the anchor fan on tensile capacity. In this setup the concrete block was moved so that the plane of one face coincides with the center of the reaction frame such that the anchor is aligned vertically (see Fig. 5). Due to debonding of the anchor fan from the concrete substrate in the very first test, the preparation procedure was subsequently modified to prevent debonding failure of the anchor fan. The target failure mode was fiber rupture at the key portion of the anchor fan as this results in the maximum capacity of the anchor. Rupture failure at the key portion is a result of the stress concentration at the bend of the fibers. The preparation method was modified to simulate the field application of an anchor fan that was splayed on a concrete column substrate. In these applications, the anchor fan is typically confined by a CFRP wrap, preventing debonding of the anchor fan from the concrete column substrate. The modified preparation procedure is summarized herein. The preparation began with sandblasting the sides of the concrete block to remove the outermost layer of cement paste to achieve a strong bond to the concrete substrate. Following the surface preparation, a groove was cut into the face of the concrete block 50 mm from the bottom edge. All concrete surfaces were cleaned to ensure a dust-free interface prior to installation of the FRP system. Two-component

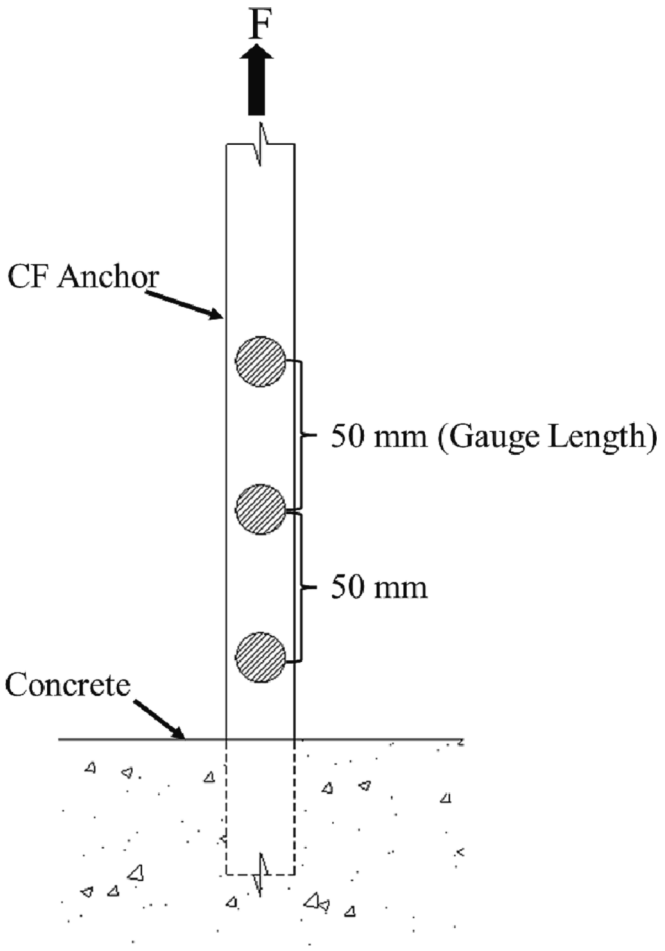

Fig. 6. Location of LED Markers on CF Anchor.

epoxy was used to prime the cleaned concrete substrate, and a thickened two-component epoxy was used to fill the voids on the concrete substrate. Then, a 610 mm wide and 1170 mm long CFRP sheet was saturated and bonded vertically to the concrete substrate as shown in Fig. 9a. A rib roller was used to remove trapped air behind the CFRP laminate. CF anchors were saturated and hung vertically to form the anchor dowel part, which will be restrained in the anchor tube as shown in Fig. 9b. The saturated CF anchor was pulled through a PVC pipe that was placed close to the top edge of the concrete block to represent the anchor hole. Once the CF anchor was in place, the anchor fibers were splayed and stretched on the CFRP laminate with a putty knife as shown in Fig. 9c. To achieve the 37° fan angle, a fan width and length of 393 mm and 533 mm was used, respectively. For the 57° fan angle, the fan width was increased to 610 mm, while the fan length remained at 533 mm. Later, a 610 mm long 25 mm diameter NSM GFRP bar was used to push the 1170 mm long vertical CFRP laminate at its mid height into the groove with thickened epoxy to anchor the CFRP laminate as shown in Fig. 9c. Then, the rest of the CFRP laminate was folded to sandwich the anchor fan as shown in Fig. 9d. Finally, a 1170 mm long single layer of transverse CFRP laminate was applied on top of the outermost vertical layer of CFRP, as shown in Fig. 9e.

2.5. Test matrix

2.5.1. Test matrix for direct tension tests

Based on communication with the manufacturers of the CF anchors, it was determined that the diameter of commercially available anchors was established by pulling dry fibers into tubes with various inner diameters. For example, to obtain a 25 mm diameter anchor, a tube with a

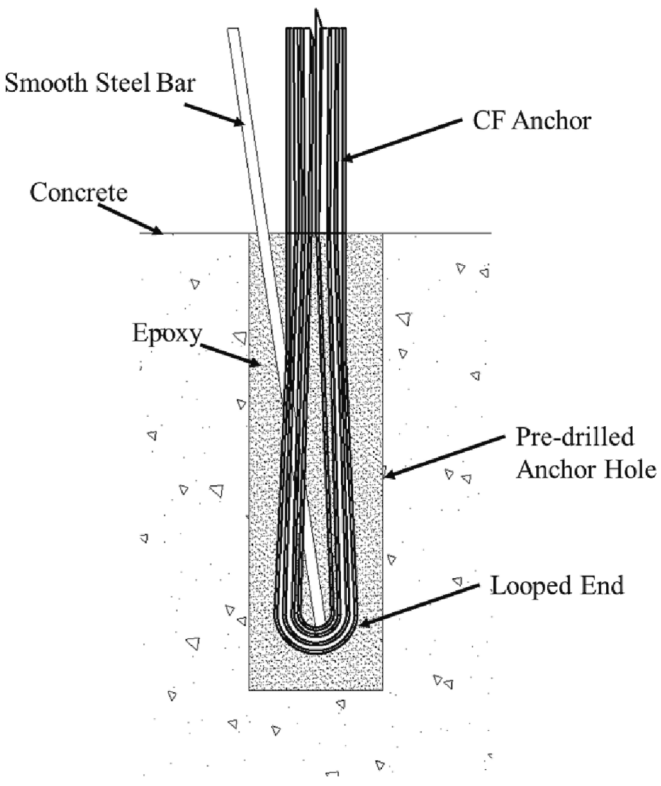

Fig. 7. Typical Installation of CF Anchors.

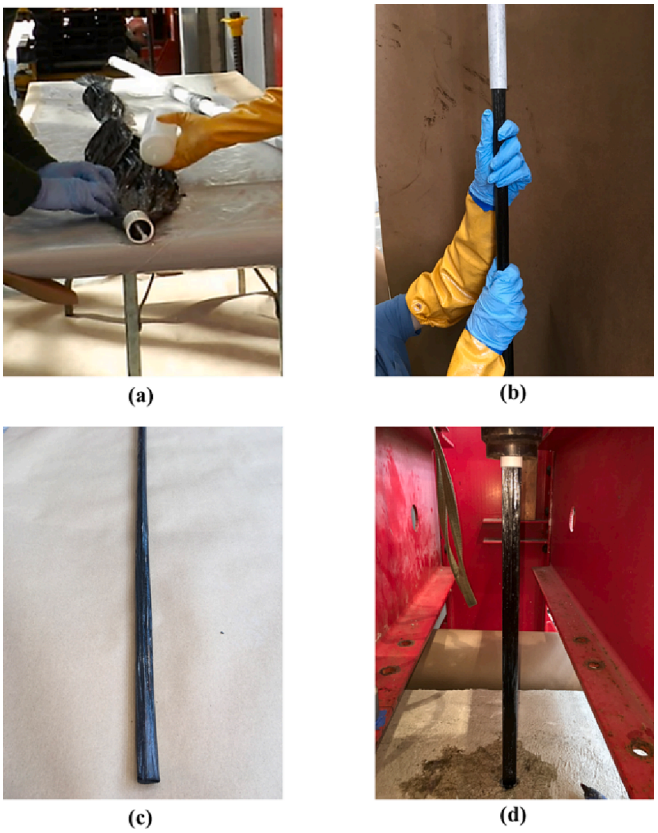

Fig. 8. Improved Anchor Preparation Procedure.

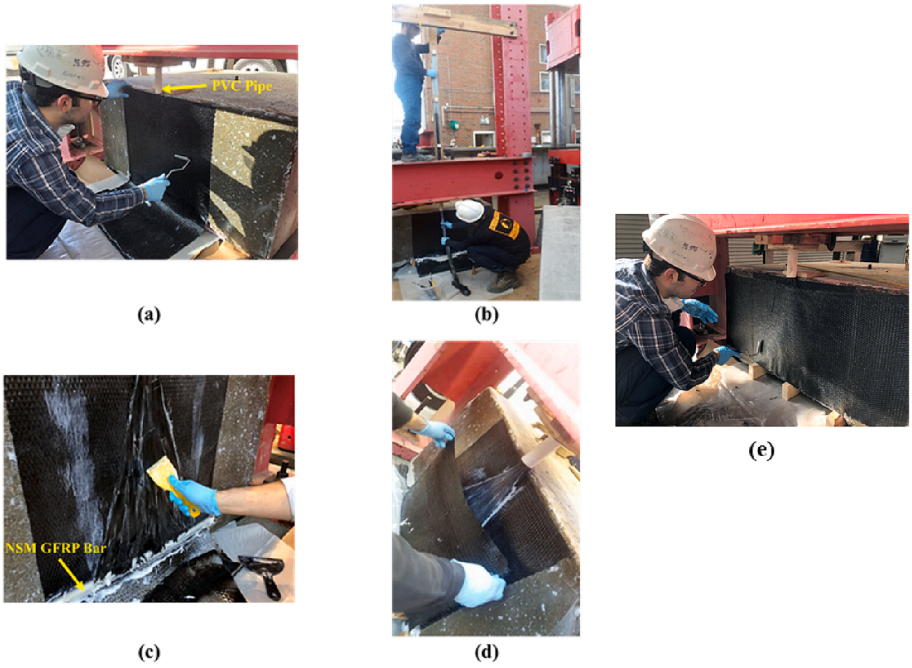

Fig. 9. The Fanned Anchor Preparation Procedure.

25 mm inner diameter is used. The amount of dry fiber that can fit into the tube determines the diameter of the anchor. Although commercially available anchor diameters were up to 38 mm at the time of testing, the largest CF anchor diameter utilized in an FRP application found in the literature was 30 mm. Therefore, 32 mm diameter anchors were selected as the largest anchor diameter in this research program. In addition, anchor handling and quality control is more difficult with increasing anchor diameter, and repair system efficiency decreases. It should be noted that an anchor could be manufactured manually using a bundle of dry fibers using the approach described above to achieve a specific diameter, as long as the capacity of the anchor is determined with representative tests. To cover a range of large anchor diameters that are commercially available, 19 mm and 25 mm diameter anchors were also included in the research program. An embedment depth of ten times the anchor diameter was used by Rutledge et al. [7] for fanned anchors. In addition, Ahmed et al. [18] showed that ten times the diameter of GFRP bars is sufficient to achieve the tensile capacity of GFRP bars. For the straight CF anchors tested in this program the pull-out anchor capacity is expected to be higher, and therefore an embedment depth at least ten times the anchor hole diameter would likely be required. It should be noted that due to the preparation method, the actual diameter of CF anchors will not be same. Therefore, using anchor hole diameter to define the anchor embedment depth is more consistent. Based on discussions with the manufacturers, the drilled anchor hole was selected to be 6 mm larger than the nominal anchor diameter. This provides sufficient clearance to install the anchor dowel while at the same time avoiding possible shear failure through the epoxy. The Anchor ID for the 16 anchors tested in this series are given in Table 1 and is of the following format: [Anchor Diameter in mm]-[Installation Procedure]-[Test Number]-[Embedment Depth as a multiple of Anchor Hole Diameter (##d_h)]. Each installation procedure is identified by a letter: "A" representing a typical field application where a smooth bar was used to push the anchor from its looped end into the anchor hole; "B" representing the anchors whose full length was pulled through a PVC pipe, cured, then embedded into the anchor hole; and "C" representing the anchors whose fibers were aligned by hand, cured, then embedded into the anchor hole. Lastly, ## is the multiplier of the anchor hole diameter (d_h) to define the anchor dowel embedment depth in mm.

Table 1
Results of Direct Tension Tests.

Anchor ID	Embedment depth (mm)	Maximum force (kN)	Nominal avg stress (MPa)	Strain (mm/mm)	Theoretical capacity (kN)	Efficiency (%)	Failure mode
19-A-1-10d_h	254	133	465	0.005	281	47	Cleavage Rupture
19-A-2-10d_h	254	87	306	0.005	281	31	Cleavage Rupture
19-B-3-12d_h	305	257	902	0.01	281	92	Cleavage Rupture
19-C-4-13d_h	330	325	1139	0.012	281	116	Splitting Rupture
19-C-5-13d_h	330	329	1155	0.013	281	117	Splitting Rupture
25-B-1-12d_h	460	254	500	0.005	500	51	Pull-out
25-C-2-12d_h	381	445	878	0.01	500	89	Pull-out
25-C-3-12d_h	381	409	808	0.01	500	82	Cleavage Rupture
25-C-4-12d_h	381	417	822	0.01	500	83	Cleavage Rupture
25-C-5-12d_h	381	449	887	0.01	500	90	Pull-out
25-C-6-13d_h	413	480	947	0.012	500	96	Pull-out
25-C-7-13d_h	413	484	955	0.011	500	97	Pull-out
32-A-1-10d_h	381	454	573	0.009	781	58	Cleavage Rupture
32-A-2-10d_h	381	245	309	0.004	781	31	Cleavage Rupture
32-B-3-11d_h	419	479	605	0.007	781	61	Pull-out
32-B-4-11d_h	419	356	449	0.0054	781	46	Pull-out

2.5.2. Test matrix for fanned anchors

The aim of this test series was to investigate the effect of fan angle on the anchor capacity. Only 25 mm diameter anchors were tested under direct tension. It is expected that similar trends would be observed for the 19 mm and 32 mm diameter anchors. The anchor fan length and anchor fan width were adjusted to obtain the desired anchor fan angle. Two fan angles were selected to investigate the impact of fan angle. As the CFRP sheet used in the testing program had a width of 610 mm, the maximum fan width to limited to 610 mm. As a result of the concrete block height and location of the groove for the NSM GFRP bar, the maximum fan length was limited to 533 mm. Thus, a maximum fan angle of 57° was obtained, which is approximately the same as the maximum fan angle of 60° reported by others in the literature. A larger fan angle can be obtained by shortening the fan length for same fan width but a larger fan angle would result in a lower anchor capacity. The minimum fan angle considered in this research was a trade-off between maximizing anchor capacity, quality control of the anchor fan installation as the anchor fan is thicker with smaller fan angle, and overlapping anchor fans of adjacent anchors when installed in a column retrofit application. Details of the seven anchors tested in this series are given in Table 2. The Anchor ID in Table 2 defines key details of the CF anchor tested according to the following format: [Fan Angle in degrees]-[Anchor Test number].

2.6. Results of direct tension tests

2.6.1. Results of straight anchors

All specimens were monotonically loaded to failure. The discussion of the results presented herein is based on the definition of efficiency introduced by del Rey Castillo et al. [13]. Efficiency is defined as the ratio of the average tensile stress of an anchor obtained experimentally to the theoretical laminate tensile rupture stress provided by the manufacturer. The average anchor tensile stress capacity is calculated by dividing the experimentally obtained maximum anchor force by the area of the anchor calculated using the nominal anchor diameter. The results of the 16 direct tension anchor tests are given in Table 1 where average tensile stress, efficiency, and strain at failure are given for the failure modes observed. Fig. 10 illustrates the three types of failures observed. Seven out of sixteen anchors failed by pull out, similar to that shown in Fig. 10a, where it can be seen that the anchor pulled from the anchor hole with a shallow concrete cone. The remaining anchors failed by one of two rupture modes. Some anchors failed in a splitting rupture mode as shown in Fig. 10b, similar to the failure observed in tension tests of pultruded GFRP bars, while other anchors failed in cleavage rupture close to the anchor hole, as shown in Fig. 10c. The latter is attributed to localized dry fibers near where the key portion of the anchor would be, or local bulging of the fibers due the installation procedure used.

Table 2
Test Matrix for Fanned Anchors.

Anchor ID	Fan Length (mm)	Fan Width (mm)	Fan Angle (degrees)	Vertical CFRP Laminate	Transverse CFRP Laminate	NSM GFRP Bar
37-A1	610	444	37	One Layer	–	–
37-A2	533	393	37	Two Layer	One Layer	Ø25 mm
37-A3	533	393	37	Two Layer	One Layer	Ø25 mm
37-A4	533	393	37	Two Layer	One Layer	Ø25 mm
37-A5	533	393	37	Two Layer	One Layer	Ø25 mm
57-A6	533	610	57	Two Layer	One Layer	Ø25 mm
57-A7	533	610	57	Two Layer	One Layer	Ø25 mm

The significance of installation method, as it relates to alignment of the fibers in the anchor dowel is evident when considering the efficiency and failure mode of the 19 mm diameter anchors. All five 19 mm diameter anchors tested failed by rupture, but the efficiency varied dramatically as a function of installation method. The efficiency increased as the alignment of the fibers in the anchor dowel improved. Installation procedure A, which most closely resembled a field application where a smooth bar is used to push the loose anchor fibers into the anchor hole from the loop end, resulted in the lowest efficiency of 47% and 31% for anchor specimens 19-A-1-10d_h and 19-A-2-10d_h, respectively. Besides significant fiber misalignment, bulging of fibers at the key portion above the anchor hole is possible. As the fiber alignment improved with different installation procedures, so did the efficiency. Anchor specimen 19-B-3-12d_h ruptured at 257 kN, yielding a 92% efficiency while anchor specimens 19-C-4-13d_h and 19-C-5-13d_h resulted in 116% and 117% efficiency, respectively. Based on the results of the 19 mm diameter anchors, it may be recommended that an embedment depth of 13d_{hole} is sufficient to achieve the theoretical tensile capacity of the anchor. Recall that the concrete strength at the time of testing for all concrete blocks was 49.6 MPa.

Except for anchor specimen 25-B-1-12d_h, 32 mm diameter anchor holes were drilled for the 25 mm diameter anchor specimens, consistent with the anchor hole diameter recommendation. Due to the available drill bit at the time of drilling the anchor hole for specimen 25-B-1-12d_h, the anchor hole diameter was 38 mm. It was found that this anchor resulted in lesser anchor capacity compared to the anchors with same anchor diameter that were embedded in the recommended 32 mm diameter anchor holes for 25 mm diameter anchors. Anchor pull out was observed at an efficiency of only 51% for specimen 25-B-1-12d_h. It must be noted that the lower efficiency is also expected to be impacted by the use of installation procedure B that, according to the results of the 19 mm diameter anchors, was somewhat less than the efficiency of anchors installed using method C. It can be seen that the efficiency of the remaining six 25 mm diameter anchor specimens increased significantly, installed using procedure C resulting in the most favorable fiber alignment condition. When an embedment depth of 13d_{hole} was used (anchor specimens 25-C-6-13d_h and 25-C-7-13d_h) the efficiency observed experimentally was very close to the theoretical tensile capacity at 96% and 97%, respectively.

Tests on the 32 mm diameter anchors were only completed on specimens prepared using the less desirable installation procedures, A and B. As a result, the experimentally determined efficiency was lower and also more variable, ranging from 31% to 61%, due to the variability of fiber alignment. The maximum embedment depth considered was also less than the 13d_{hole} condition met for the 19 and 25 mm diameter anchors.

Fig. 11 is a graphical representation of the efficiency of all the anchors tested in direct tension. For ease of comparison, each installation procedure is represented by a color, and each failure mode is represented by a different symbol. Red represents installation procedure A, blue represents procedure B, and green represents procedure C. It is clear from the efficiencies determined experimentally for the 19 mm diameter anchors, the average anchor tensile stress at failure increases significantly with improved fiber alignment. It also appears for the 19 and 25 mm diameter anchors produced with the ideal installation procedure C, that the variability of average anchor tensile stress at failure is less. Consistent with the observation by others, the trend of reducing anchor efficiency with increasing nominal diameter can be seen in Fig. 11. This behavior is explained by the shear lag phenomenon, as observed in tension tests of pultruded GFRP reinforcing bars embedded in concrete [19 20]. The tensile force applied to a large-diameter CF anchor embedded in a concrete anchor hole is transferred to the fibers in the cross-section by the resin matrix. Hence, the outermost fibers are stressed the most and a nonuniform stress distribution through the cross-section develops, resulting in a lower average tensile stress at failure.

Fig. 10. Failure Modes of Straight CF Anchors: a) Pull-out b) Splitting Rupture c) Cleavage Rupture.

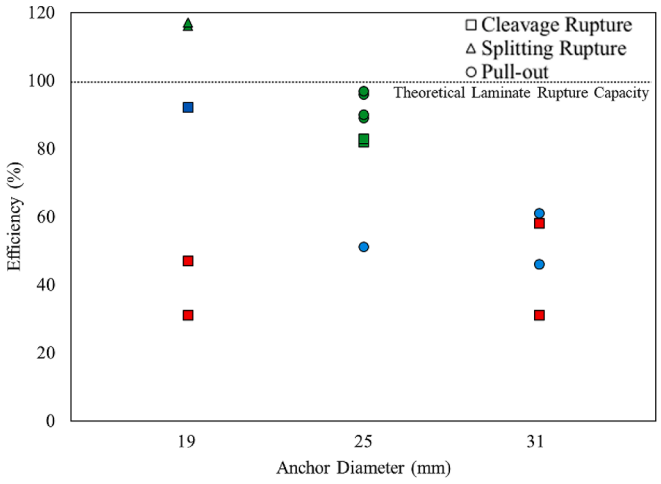

Fig. 11. Efficiency of Anchors Tested in Direct Tension.

Table 3
Test Results of Fanned Anchors.

Anchor ID	Fan Angle (degrees)	Force (kN)	Failure Mode	Efficiency (%)
37-A1	37	169	D	34
37-A2	37	271	D	54
37-A3	37	257	D	51
37-A4	37	266	D	53
37-A5	37	302	D	60
57-A6	57	307	S/D	61
57-A7	57	249	S/R	50

D: Debonded, S: Split Fibers, R: Rupture.

2.6.2. *Fanned anchor tests results*

All fanned anchors were loaded monotonically in tension until failure. The results of each anchor test is presented in Table 3, where efficiency is again defined as the ratio of the average tensile stress of an anchor obtained experimentally to the theoretical laminate tensile rupture stress provided by the manufacturer.

The failure modes observed in this test series include fiber rupture, splitting, and debonding, as illustrated in Fig. 12. The very first fanned anchor tested, 37-A1, did not contain any level of confinement and failed by debonding of the anchor fan at 169 kN. The efficiency of this anchor was only 34%, which is expected to be a lower bound result given that no mechanism was provided to delay, or prevent, anchor fan debonding. In an attempt to achieve the rupture capacity of the fanned anchors the test setup was modified, as described previously, by providing additional longitudinal and transverse fibers spanning beyond the anchor fan. Following modification of the test setup, the efficiency of fanned anchor 37-A2 increased to 54%, with debonding occurring at a tensile force of 274 kN. For specimens 37-A3 and 37-A4, the tensile force continued to increase beyond the initiation of debonding until local failure of the concrete at the top edge of the groove of the NSM GFRP bar, as can be seen near the bottom of Fig. 12a. The observed debonding failures were restricted to the width of the anchor fan because stress was only transferred to the vertical fibers via the anchor fan. Therefore, splitting of the vertical CFRP laminate was observed near both edges of the anchor fan, as can be seen in Fig. 12a. For a circular column application where transverse CFRP laminates wrap around the column to confine the anchor fan, this debonding failure mode would likely be delayed or prevented. Hence, the anticipated capacity of a well confined fanned anchor is expected to be higher than that observed in this test series.

For specimens 57-A6 and 57-A7, debonding or rupture of anchor fibers at the key portion was observed after fiber splitting. It appears that for anchors with a fan angle approaching 60°, rupture of fibers at the key portion is likely due to the concentration of stress at the sharp bend. The installation procedure of the key portion also likely played a role in this observed failure behavior. Anchor fibers split as the fibers at the key portion were not confined as would be the case in a field application where the dowel is embedded in a drilled hole in the concrete. Although splitting cracks occurred and propagated through the anchor dowel of the anchors with smaller fan angles, the splitting crack width was small and did not lead to splitting failure as fibers were aligned more vertically. Also, the epoxy filling the drilled hole near the key portion may work to improve the stress distribution locally. Thus, it would be recommended to develop a future test setup that better represents an anchor hole filled with epoxy.

The efficiency of the tested anchors given in Table 3 is represented graphically in Fig. 13. For reference, the results of the six 25 mm diameter straight CF anchor tests using installation procedure C (see Table 1), representing a fan angle of 0°, are also included in Fig. 13. The data point identified by the × for the 37° fan angle is the test that did not include the beneficial effect of confinement. As a result, it is expected to represent a lower bound capacity, and is not considered in the following

(a) (b) (c)

Fig. 12. Observed Failure Modes of Fanned Anchors a) Debonding b) Fiber Rupture c) Splitting.

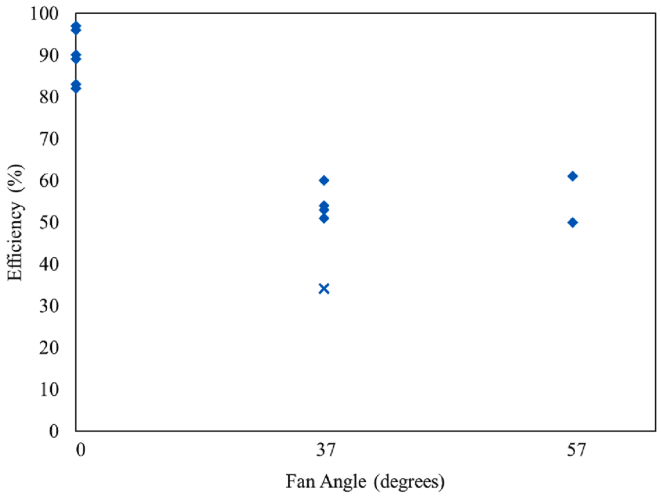

Fig. 13. Efficiency Distribution of Fanned Anchors.

discussion. The impact of the anchor fan on the efficiency of an anchor is clearly seen in Fig. 13. The average efficiency of the four 25 mm diameter straight CF anchor tests with embedment depth of $12d_h$ is 86% with standard deviation of 3.53. For comparison, the average efficiency of the five 25 mm diameter fanned anchor tests (not including 37-A1) is 55% with a standard deviation of 4.22. There does not appear to be any difference in fanned anchor efficiency for the fan angles considered, ranging from 37° to 57°. However, the presence of the anchor fan reduced the capacity of the straight anchor by 36%. It should be noted that the confinement of the anchor fan, enhancing the resistance to debonding, will be more effective in a circular column application.

3. Columns bending tests with a single CF anchor

3.1. Test setup for columns with a single CF anchor

As the columns for this series of tests were obtained from a previous research study [21], the test setup used in the previous research study was adopted with only slight modifications. As the aim of this series of column tests was to examine the behavior of large diameter CF anchors under bending conditions, the constant axial load that was applied to the original columns was not included in this test setup. A schematic of the test setup is shown in Fig. 14. The column specimen was tied to the strong floor with post-tensioning bars at the four corners of the rectangular footing, and a 13 mm thick hydrostone layer was cast under the footing to ensure a uniform and level interface with the strong floor. The lateral load was applied to the column cap with a 490 kN actuator with a ± 250 mm stroke capacity, attached to a strong wall through high strength rods. The lateral load, lateral displacement, and strain at the repair region of the test specimen were recorded during testing. The lateral load was measured via a load cell integrated with the actuator. The lateral displacement was measured using a string pot attached to the mid-height of the column cap, 2.4 m above the top of the column footing. To obtain strain data in the repair region, 10 non-contact optical measuring system LED markers were placed in a single-column configuration at a nominal spacing of 50 mm for the first column test, C-1, as shown in Fig. 15a. In order to also obtain hoop strain data, 20 LED markers were placed in a two-column configuration shown in Fig. 15b for the remaining two tests, C-2 and C-3. In addition, a digital image correlation (DIC) system was used to record the full strain field over a larger area of the repair region. High resolution digital cameras were used to capture images of a high contrast random speckle pattern applied to the surface of interest that are subsequently used to obtain continuous strain fields.

3.2. Preparation of column bending test specimens

The specimens used in the column bending test series were obtained from another research study where circular RC columns with high-strength internal reinforcing steel were tested under cyclic loading [21]. The columns were 610 mm in diameter with 16 No. 6 (19 mm diameter) A706 Grade 80 longitudinal bars evenly distributed around the column, and a No. 3 (10 mm diameter) A706 Grade 80 spiral transverse reinforcement, with varying pitch. The original columns were loaded until three extreme longitudinal bars were fractured, as shown in Fig. 16. A single CF anchor was installed on the extreme faces of the columns where fractured bars existed. In this way the CF anchor is subjected to tension as a result of bending. In addition to the fractured longitudinal bars from the original column test, buckled bars shown in Fig. 16 were cut so that only the straight bars near mid-depth of the column remained intact to maintain stability of the column. In this way, the tension force developed in the anchors would primarily be resisting the moment in the column section due to bending. Loose concrete was removed and concrete behind the bars was chipped away as shown in Fig. 16. This was done to ensure that the grout cast to restore the original column cross-section would bond with the internal reinforcing steel. Pressurized water was used to clean the dust and debris from the column surface. As the fractured and buckled bars pushed the transverse steel outside the original section of the column, the diameter of the repaired region was enlarged with a high-strength non-shrink grout to 660 mm to ensure that the longitudinal and transverse reinforcing steel had

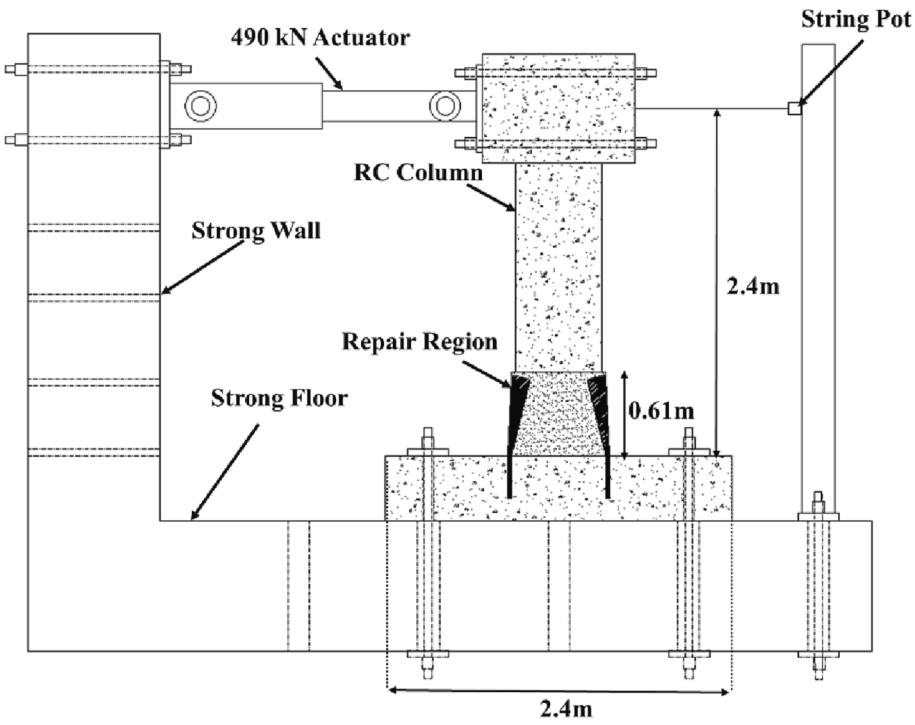

Fig. 14. Test Setup for Column Bending Test.

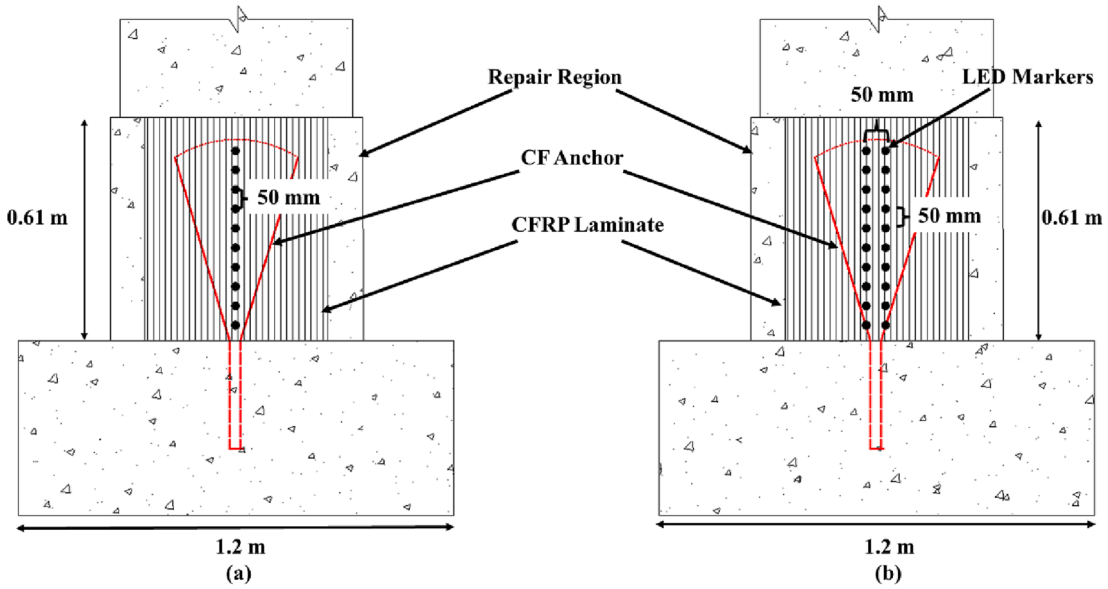

Fig. 15. Non-Contact Optical Measuring System LED Marker Configuration a) Column C-1b) Columns C-2 and C-3.

sufficient cover. The average grout compressive strength on the day of the testing was 57.2 MPa, 58.6 MPa, and 59.3 MPa for columns C-1, C-2, and C-3, respectively.

To restore the circular column cross-section a commercially available flexible board was used. The flexible board was set around the column as shown in Fig. 17a. Then, a flowable high-strength non-shrink grout was poured into the form to restore the cross-section. The smooth surface (Fig. 17b) after the form was removed was roughened with a needle gun as shown in Fig. 17c. Later, an anchor hole was drilled with an impact hammer drill, as can be seen in Fig. 17d. The edge of the anchor hole was rounded (see Fig. 17e) to ensure that the anchor fibers at the key portion do not get damaged by sharp edges. Finally, the inside of the anchor hole was brushed to remove any loose debris, as shown in Fig. 17f. Before moving the columns inside the laboratory prior to testing, all surfaces were cleaned using pressurized air.

One day before installation of the FRP system on the RC column, a short length of the loop end of the CF anchor was cured in a PVC pipe to form a circular cross-section that can be inserted into the anchor hole. The formed CF anchor end, shown in Fig. 18a, provides an effective way of pushing the CF anchor into the anchor hole. The two-component epoxy was mixed following the manufacturer's recommendations, and the repair region was primed with the epoxy, and the CFRP sheet (columns C-2 and C-3 only) was impregnated and applied to the concrete surface, as shown in Fig. 18b. The remainder of the dowel part of the CF anchor was saturated with epoxy, and the anchor hole was partially filled with the remaining epoxy. The CF anchor was pushed into the

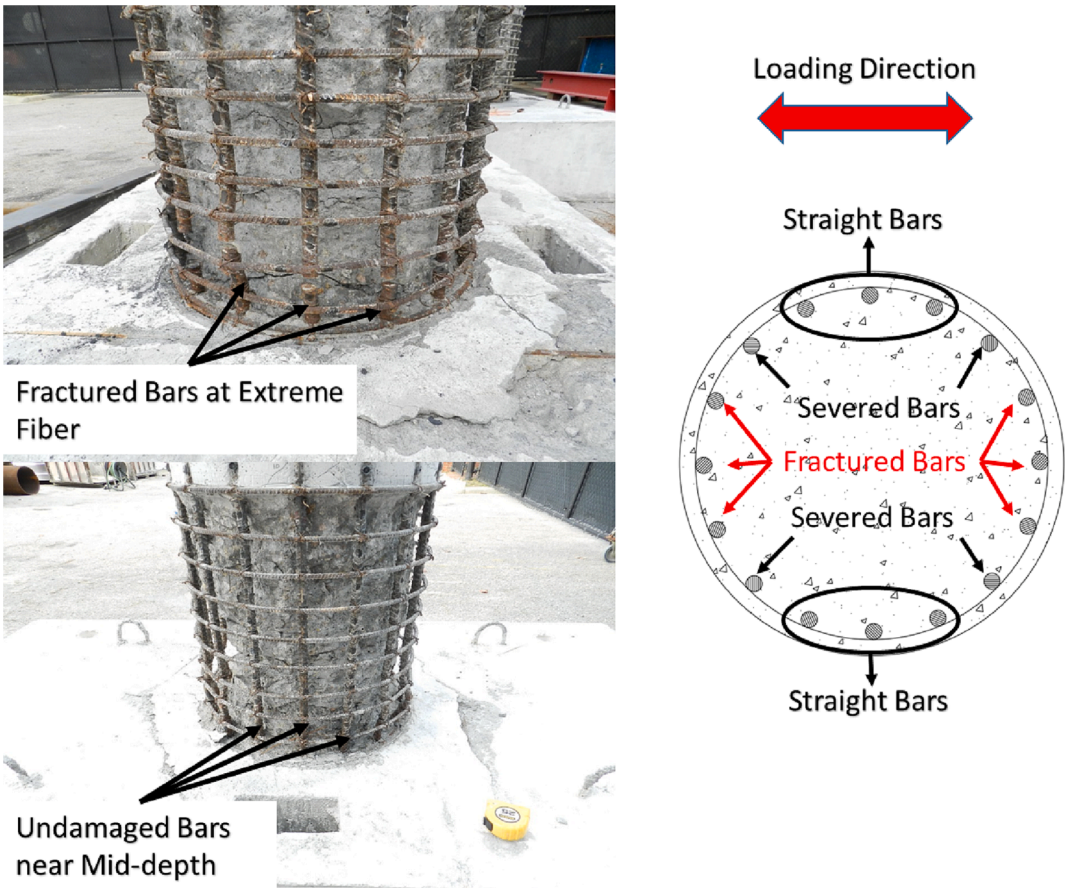

Fig. 16. Condition of Tested Columns.

anchor hole with a smooth steel bar as shown in Fig. 18c, and the CF anchor fan fibers were splayed onto the CFRP laminate surface. The CF anchor fan fibers were saturated with epoxy using a bristle brush as shown in Fig. 18d. A putty knife (see Fig. 18e) was used to stretch the anchor fan fibers to ensure no bulging at the key portion of the anchor. It was observed that saturating the CF anchor fan fibers with a bristle brush left some dry fibers. Therefore, for subsequent installations, the anchors were fully saturated with epoxy before splaying the anchor fan fibers. Unsaturated fibers will reduce the anchor capacity and result in a premature failure (as discussed later with specimen C-2-A2-254). For columns C-2 and C-3, transverse CFRP laminates were wrapped around the column as shown in Fig. 18f. A ribbed roller was used to remove trapped air from behind the CFRP laminates.

3.3. Test matrix for column specimens

Three RC columns were utilized to investigate the behavior of CF anchors under column bending. All of the anchors tested in this series had a nominal 25 mm diameter. The test matrix shown in Table 4 was developed to investigate column bending on CF anchor behavior. The Anchor ID in Table 4 defines key details of the column anchor tests according to the following format: [C: Column]-[Column Number]-[Anchor Test Number]-[Anchor Hole Depth in mm].

In the first test (C-1-A1-330) the anchor was installed into a 330 mm deep anchor hole, and splayed directly on the concrete substrate using a fan width of 380 mm and fan length of 559 mm, resulting in a fan angle of 37°. The anchor hole diameter was 32 mm for all anchors tested in this series. After testing the first anchor monotonically under column bending, the second anchor on the diametrically opposite face was installed. The second test (C-1-A2-355) was modified by installing the anchor into a 355 mm deep anchor hole and splaying the anchor fan onto a single layer of vertical CFRP laminate that was bonded to the concrete substrate. The width of the anchor fan was 380 mm and the fan length was 483 mm, resulting in a fan angle of 43°. The intent was to splice the anchor fan with a CFRP sheet with fibers oriented in the longitudinal direction representing a typical FRP flexural strengthening application. The embedment depth was not the same for every test depending on the anchor hole location relative to the internal steel reinforcement of the footing. The fan length of the second anchor was reduced as the bond between the anchor fan and the CFRP laminate was expected to be stronger than that of the anchor fan and the concrete substrate. For the second column tests (C-2-A1-381 and C-2-A2-254), two CF anchors were installed (one at each extreme face of the column) into 381 mm and 254 mm deep anchor holes, and the anchor fans were splayed directly on the concrete substrate with an anchor fan width of 380 mm and an anchor fan length of 559 mm, resulting in a fan angle of 37°. Both anchors were installed on the same day. Following the installation of both anchors, the repair region was wrapped with three layers of hoop fibers designed to prevent anchor fan debonding observed in the C-1 column tests. A detailed discussion of the design of the CFRP wrap is given in the following section. The anchor fans were sandwiched between two vertical CFRP laminates and wrapped with three layers of hoop fibers for the third column tests (C-3-A1-330 and C-3-A2-280). The embedment depth of these anchors was 330 mm and 280 mm, respectively, and the fan width and fan length were 380 mm and 559 mm for both anchors, again resulting in a fan angle of 37°. Based on the observation from the C-2 column tests, the vertical CFRP laminates were deemed to be necessary as large flexural cracks in the grout substrate due to the fractured steel reinforcing bars led to an undesired failure mode.

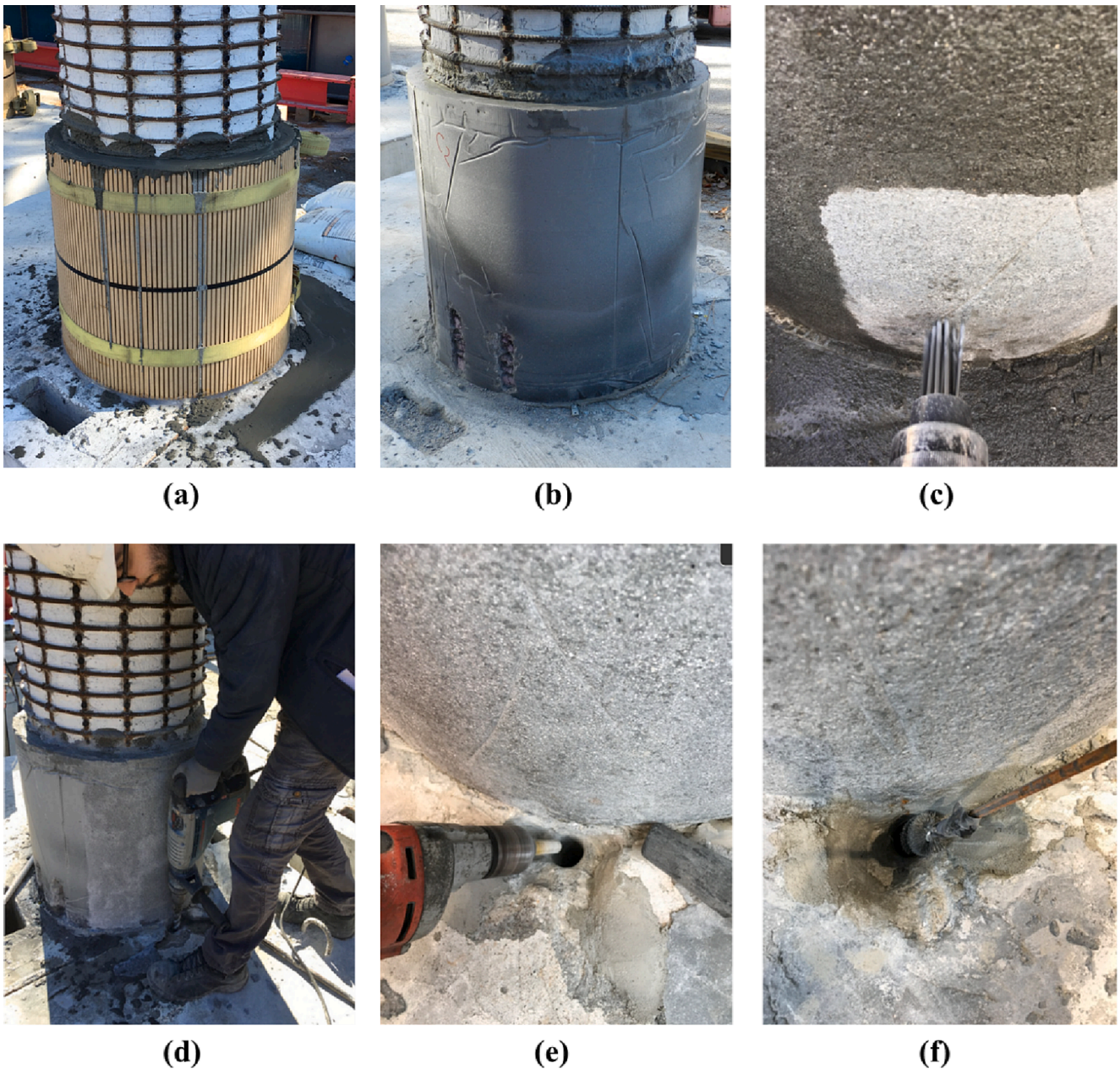

Fig. 17. Preparation of Cover Concrete: a) Flexible Form with High-Strength Non-Shrink Grout, b) Restored Cross Section, c) Surface Roughening, d) Anchor Hole Drilling, e) Anchor Hole Edge Rounding, f) Brushing.

3.4. Design consideration for hoop fibers

Confining the CF anchor fan with hoop fibers is a practical and convenient way of preventing debonding failure of the anchor fan for the application considered in this test series. The length of vertical CFRP laminates, or the anchor fan, are limited in plastic hinge relocation applications so as not to over strengthen the column, increasing demands on other structural elements of the system. The design concept suggested by Rasheed et al. [22] for the design of U-wraps to anchor EB longitudinal FRP for flexural strengthening via a clamping force mechanism was adopted in this research. Dilation of the debonding crack at the FRP-to-concrete interface mobilizes the U-wrap resulting in a force normal to the debonding plane restraining the propagation of the debonding crack. In the limit, if the frictional force developed along the debonding crack is sufficiently large it will be possible to achieve the rupture strain limit of the longitudinal FRP.

In the repair of plastic hinge regions in damaged RC columns, the CF anchor fan is sandwiched between vertical CFRP laminates that are bonded to the concrete surface and wrapped with hoop fibers. The vertical fibers transfer axial tensile forces due to column bending from the column to the footing through the CF anchor across the interface. Transverse fibers in the hoop direction from a CFRP wrap will have the tendency delay, or prevent, premature debonding of the vertical CFRP at the concrete substrate interface. The magnitude of the clamping force provided by the CFRP wrap is a function of the number of layers of hoop fibers, and may be designed by adapting the procedure proposed by Rasheed et al. [22]. With increasing lateral column deformation, the axial tension force in the CF anchors also increases until such time that debonding initiates at the concrete interface. The CFRP must slip relative to the concrete as the debonding crack propagates, which must also be accompanied by dilation, the widening of the debonding crack. This mechanism engages the CFRP wrap and develops tensile hoop strain that is limited by the rupture strain capacity of the transverse fibers. The confinement stress that develops as a result of the tension in the CFRP

Fig. 18. CFRP Application a) Cured Loop End b) CFRP Laminate Application c) CF anchor Application and Splaying of Anchor Fan Fiber d) Anchor Fan Fiber Saturation e) Stretching Anchor Fan Fiber to Form Anchor Fan f) Transverse Wrap.

Table 4
Test Matrix for Anchors Tested under Column Bending.

Anchor ID	Fan Width (mm)	Fan Length (mm)	Anchor Embedment Depth (mm)	Transverse CFRP Laminate	Vertical CFRP Laminate
C-1-A1-330	380	559	330	–	–
C-1-A2-355	380	483	355	–	One Layer
C-2-A1-381	380	559	381	Three Layers	–
C-2-A2-254	380	559	254	Three Layers	–
C-3-A1-330	380	559	330	Three Layers	Two Layers
C-3-A2-280	380	559	280	Three Layers	Two Layers

wrap provides a frictional resistance along the debonding crack that will resist the slip. Depending on the magnitude of the frictional resistance developed, the propagation of the debonding crack may be prevented so that the rupture capacity of the anchor will be achieved and control failure. If the frictional resistance developed exceeds the tensile capacity of the CF anchor, then debonding would be prevented resulting in a rupture failure mode, achieving the maximum capacity of the fanned anchor. Two parameters are required to design the number of layers of hoop fibers, namely, the coefficient of friction along the cracked concrete debonding interface and the CFRP hoop fiber rupture strain limit. Rasheed et al. [22] used a coefficient of friction of 1.4. In this research a more conservative coefficient of friction of 1.0 was used as the debonding failure plane through the high-strength non-shrink grout used to restore the concrete section was expected to have a smoother cracked surface due to the absence of coarse aggregate. The design strain limit of the CFRP hoop fibers was taken as 0.0058, based on research by Harries and Carey [23].

3.5. Column tests results

Three columns were tested under a single monotonic push and pull cycle until the CF anchor on diametrically opposite faces of the column failed in tension. Observations and results of each anchor test are presented in the following sections for each of the three columns tested.

3.5.1. Column C-1

When the top of the column reached 20 mm of lateral displacement at a lateral load of 102 kN in specimen C-1-A1-330, the CF anchor fan suddenly debonded from the grout substrate as shown in Fig. 19a. The observed debonding failure was initiated due to formation of a flexural crack in the grout substrate near the column-footing interface, as identified in Fig. 19a. Following the formation of the flexural crack in the grout due to column bending, the debonding crack at the anchor fan-grout interface initiated and propagated as the flexural crack widened, ultimately leading to complete debonding of the CF anchor fan. For specimen C-1-A2-355, the CFRP laminate debonded from the grout substrate at the same column lateral load and displacement level. The debonded CFRP laminate was contained within the width of the anchor fan, as can be seen in Fig. 19b. The CFRP laminate bonded between the CF anchor fan and the grout substrate did not improve the bond as the same debonding mechanism developed. The vertical strain field over the anchor fan obtained using the DIC, as well as the vertical strain distribution along the center-line of the anchor fan using the non-contact optical measuring system data, are shown for the two anchors tested on Column C-1 in Fig. 20. The strain distributions shown in Fig. 20 were taken just prior to failure, at a lateral load on the column of 102 kN. It can be seen that the maximum strain is located in the region near the key portion of the anchor fan above the footing interface. For specimen C-1-A1-330 the local maximum recorded strain is in the range of 0.008–0.009 according to the DIC data, and approximately 0.005 according to the non-contact optical measuring system data. For specimen C-1-A2-355, the maximum recorded DIC strain is between 0.0065 and 0.007, and 0.009 according to the non-contact optical measuring system data. As expected, the strain varies from a maximum near the column-footing interface at the key portion of the anchor fan to zero at the top free edge of the anchor fan. The strain does not vary uniformly along the length of the anchor fan due to the local effects of cracking of the grout substrate behind the anchor fan and nonuniform thicknesses of grout remaining attached to the debonded anchor fan.

The height of the vertical CFRP laminate used in specimen C-1-A2-355 was 610 mm and is limited by the extent of the plastic hinge region of the repaired column, as discussed in previous research [7]. However, extending the vertical CFRP laminate further would not have prevented the observed debonding failure of the anchor fan. The most effective way to delay, or prevent, debonding failure of the anchor fan, especially in a circular column application, is to confine the system with a transverse CFRP wrap, as discussed in the following section.

3.5.2. Column C-2

Using the approach described in Section 3.4, three layers of hoop carbon fibers were applied based on the average straight anchor capacity of 445 kN obtained from the straight anchor test results. A conservative design procedure was followed, regardless of fan angle, to prevent anchor fan debonding. It should be noted that in this column test the anchor fan fibers were directly bonded to the grout substrate. That is, no vertical CFRP fibers were provided as in specimen C-1-A2-355. For specimen C-2-A1-381, the maximum lateral load applied to the top of the column was 169 kN at a lateral displacement of 37 mm when the anchor ruptured near the column-footing interface, as can be seen in Fig. 21a. Hence, wrapping the anchor fan with hoop fibers was effective in preventing debonding, enabling the anchor to develop its rupture capacity. Horizontal splitting parallel to the hoop fiber direction was observed, as can be seen in Fig. 21b, coinciding with the location of the flexural cracks in the grout substrate from column bending. It is observed that the splitting cracks did not propagate where the wrap overlapped the anchor fan fibers. The second anchor, C-2-A2-254, at the diametrically opposite face of the column failed prematurely due to a flaw in the installation of the anchor at a maximum column lateral load of 67 kN and a lateral displacement of 8 mm. Although this anchor was exposed to compression forces during the test of C-2-A1-381, compression is not considered to be the primary reason for the premature failure. With increasing post-peak lateral column displacement is was possible to observe that dry fibers of the anchor fan where being pulled out at the location of the flexural crack in the grout due to column bending, as can be seen in Fig. 21c. Hence, the premature failure observed in this test was largely due to improper saturation of the anchor fan fibers during

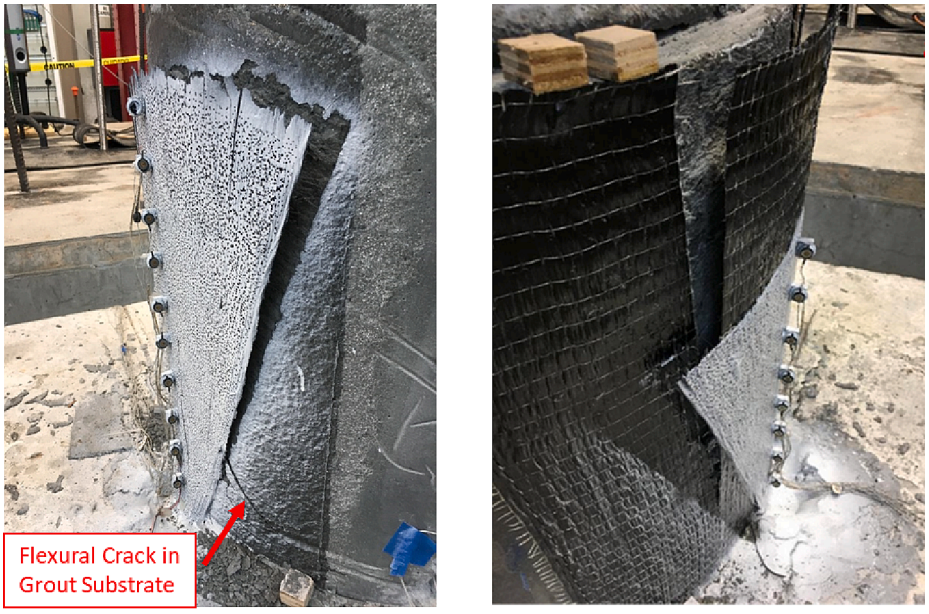

Fig. 19. Failure of CF Anchor in C1 a) C-1-A1-330b) C-1-A2-355.

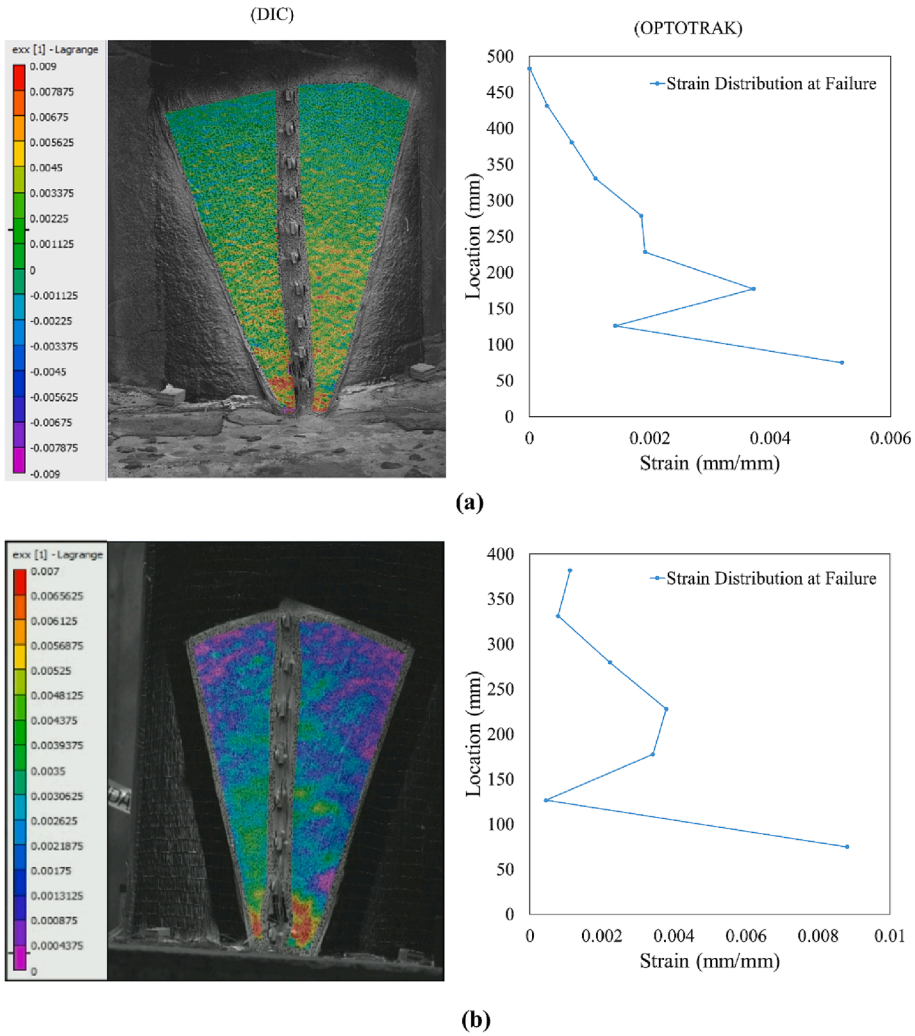

Fig. 20. Vertical Strain Distribution for Specimens: a) C-1-A1-330b) C-1-A2-355.

installation.

The strain distribution on the surface of the CFRP wrap was recorded using both DIC and non-contact optical measuring system for specimen C-2-A1-381. The concentration of vertical strain just prior to failure, at lateral column load of 169 kN, can clearly be seen in Fig. 22. These locations coincide with those of flexural cracks in the grout due to column bending near the maximum moment region above the column-footing interface, and at the top free edge of the anchor fan, located 559 mm from the top of the footing.

The hoop strain was also calculated using only the non-contact optical measuring system data shown in Fig. 23, just prior to failure when the lateral column load was 169 kN. The maximum recorded hoop strain from the non-contact optical measuring system data was approximately 0.007, which is larger than the design strain limit used (0.0058) however, no hoop fiber rupture was observed. It is worth noting that the maximum recorded hoop strain was localized at the key portion of the anchor just above the top of the footing. Over the remainder of the height of the anchor fan, the hoop strain was less than half of the adopted design strain limit. It may be concluded that the adopted design strain limit and coefficient of friction could be used to conservatively design the number of hoop fiber layers. Certainly, more tests with different anchor fan configurations and anchor diameters are needed to obtain a robust design procedure.

3.5.3. Column C-3

The two anchors designed for Column C-3, specimens C-3-A1-330 and C-3-A2-280, were intended to represent the most realistic column strengthening or repair application. For each anchor, the anchor fan was sandwiched between two layers of vertical CFRP laminates. The first layer of vertical CFRP laminates was bonded directly to the grout substrate. The anchors were then installed and the anchor fans splayed onto the surface of the first layer of vertical CFRP laminate. The second layer of CFRP laminate was then applied and finally, the three layers of hoop fibers applied to confine the entire system. It was expected that the vertical CFRP fibers will prevent the horizontal splitting of the hoop fibers at the location of flexural cracks in the grout due to column bending, resulting in a more uniform stress distribution over the anchor fan. The failure of specimen C-3-A1-330, shown in Fig. 24a, was anchor rupture at the key portion at a lateral load of 115 kN and a lateral displacement of 32 mm at the top of the column. The difference in applied load compared to that of specimen C-2-A1-381 is largely attributed to the variability of anchor rupture capacity, which is sensitive to fiber alignment in this realistic application. Specimen C-3-A2-280 ruptured at a lateral load of 88 kN and a lateral displacement of 25 mm. It should be noted that this anchor was in a state of compression while specimen C-2-A1-381 was being tested. Rupture failure of anchor C-3-A2-280 was slightly above the key portion as shown in Fig. 24b.

The vertical and hoop strain was measured on the surface of the CFRP wrap for specimen C-3-A1-330, and shown in Fig. 25a and 25b, respectively, just prior to rupture failure at a lateral column load of 115 kN. It can be seen that the vertical strain approaches zero at the location where the top of the anchor fan ends, and increases more uniformly

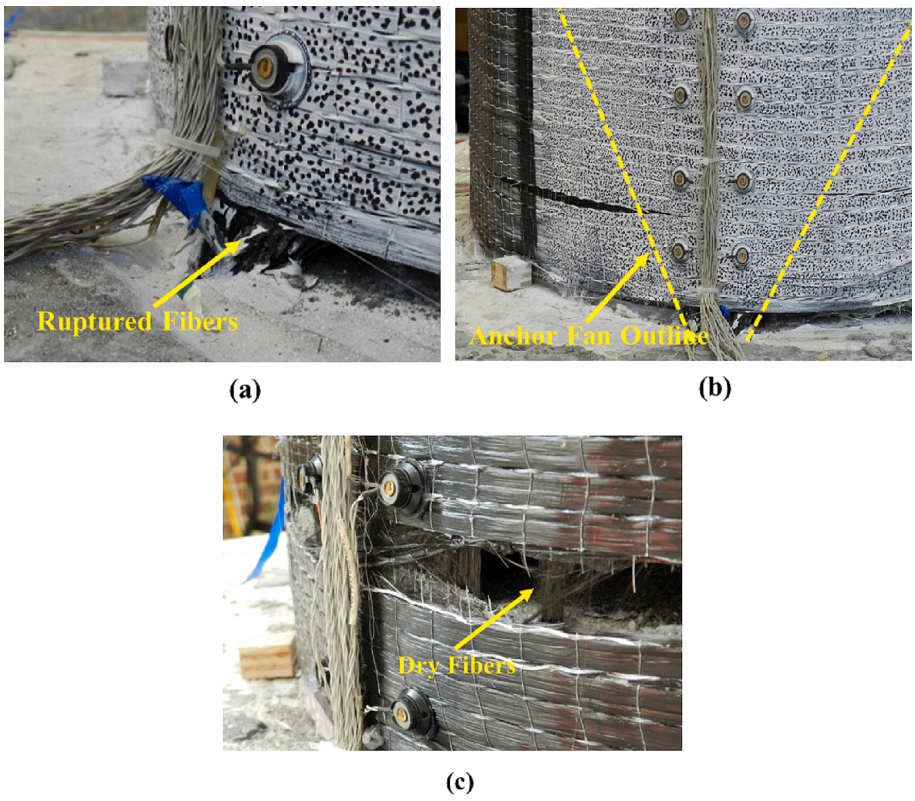

Fig. 21. Anchor Failure in Column C-2 a) Anchor Rupture (C-2-A1-381) b) Splitting of Hoop Fibers (C-2-A1-381) c) Dry Fibers Pulling Out (C-2-A2-254).

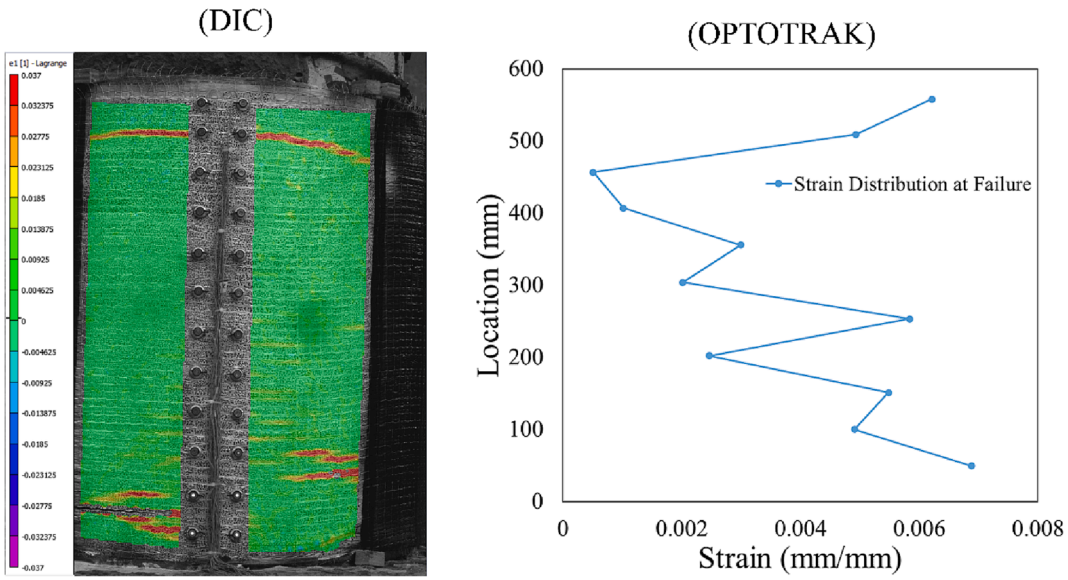

Fig. 22. Vertical Strain Measured on the Hoop Fibers.

towards the footing interface as no hoop fiber splitting was observed. The maximum measured vertical strain calculated using non-contact optical measuring system data was 0.0038, and the DIC recorded maximum vertical strain was between 0.004 and 0.005. From Fig. 25b, it can be seen that the hoop fiber strain along with the height of the repair region is less than 0.001, except locally near the bottom of the hoop fibers at the footing interface. There, the maximum measured hoop strain using non-contact optical measuring system data was 0.0035, whereas DIC yielded a maximum recorded hoop strain between 0.0037 and 0.004. Here again it may be concluded that the design approach adopted for the hoop fibers is conservative as debonding of the anchor fan was effectively prevented and failure was controlled by rupture of the anchors near the key portion. In addition, the maximum measured hoop strain was less than the adopted hoop rupture strain limit.

4. Conclusions

This paper presents the result of an experimental program that investigated the behavior of commercially available CF anchors with diameters greater than 19 mm. Although it was not possible to propose a

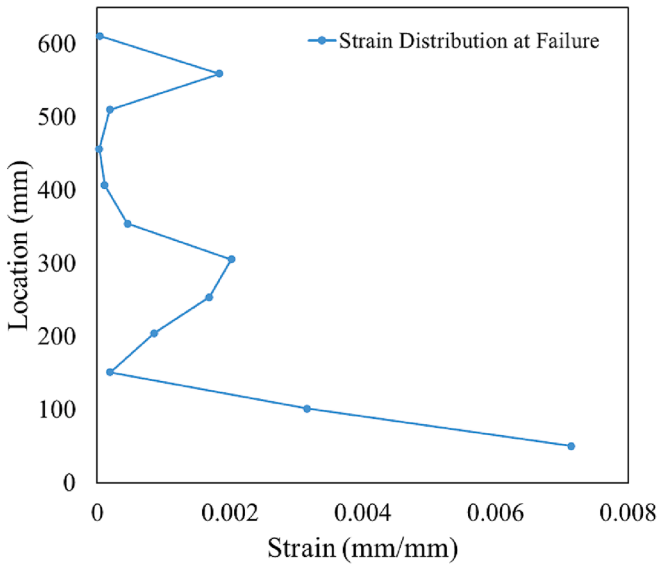

Fig. 23. Hoop Strain at Failure.

generic design equation to predict the tensile capacity of large diameter CF anchors due to the limited number of tests conducted, an improved understanding of the behavior of large diameter CF anchors was possible. Recall that efficiency in the context of anchor capacity in this paper is defined as the ratio of the average tensile stress at failure determined experimentally (and using the nominal anchor diameter) to the laminate tensile rupture stress (as provided by the manufacturer). The conclusions drawn from the test series presented in this paper are as follows:

4.1. Straight anchor test series (19, 25, and 32 mm diameter anchors)

- Quality control of the anchor installation, particularly in terms of fiber alignment, is of critical importance affecting both the failure mode and tensile capacity of the anchor. Even under laboratory conditions, variability of results were higher and efficiency as much as 50% less with increasing fiber misalignment depending on the installation procedure used.
- It is recommended to use a drilled anchor hole diameter, d_h, 6 mm larger than the nominal anchor diameter for large diameter CF anchors. When an oversized anchor hole (38 mm diameter) was drilled for one of the 25 mm diameter anchors tested, the maximum tension force achieved for that anchor was in the order of 40% less than that of the other 25 mm diameter anchors tested with the same embedment depth.
- For consistency, embedment depth is defined as a function of anchor hole diameter, d_h. Embedment depths ranging from 10 to 13 times d_h were considered in this test series. With optimum fiber alignment, the 19 mm diameter anchors achieved 100% efficiency when using an embedment depth of $13d_h$ in concrete with a compressive strength of 49 MPa. Under the same conditions, the 25 mm diameter anchors tested achieved 96% efficiency. For the 32 mm diameter anchors, the maximum recorded efficiency was 61%, but that was with an embedment depth of only $11d_h$ and without the optimum fiber alignment.
- The same size effect observed in pultruded Glass FRP reinforcing bars, where the average stress at tensile rupture reduces with increasing bar diameter (due to the shear-lag effect), is present in large diameter CF anchors.

4.2. Fanned anchor test series (25 mm diameter anchors)

- Fan angles of 37° and 57° were considered in this test series. It is recommended to use fan angles within this range. For fan angles greater than 57° it is expected that premature fiber rupture will occur at the key portion of the anchor due to the sharp change of geometry, reducing the efficiency of the anchor. For fan angles less than 37°, the anchor fan will be thicker and quality control during installation will be more difficult, resulting in more variable anchor efficiency.
- Without any confinement of the anchor fan, debonding of the anchor fan occurred at an efficiency of only 34% for an anchor with a 37° fan angle. This is expected to be a lower bound capacity and demonstrates the need to provide confinement of the anchor fan to achieve the maximum potential of the anchor in a direct tension application.
- When some level of confinement is provided to help delay debonding of the anchor fan, the efficiency achieved was in the order of 55%. Debonding remained the failure mode for anchors with a fan angle of 37°. For those anchors with a fan angle of 57°, signs of fiber rupture were observed at the key portion of the anchor.
- Overall, the presence of the anchor fan reduced the efficiency of the anchor, compared to that of the companion straight anchor, by 36%. However, confinement of the anchor fan by an FRP wrap in a column application will be more effective in delaying debonding compared to the confinement provided in this test series.

4.3. Column bending test series (25 mm diameter anchors)

- All anchors were installed with a 37° fan angle in a 32 mm diameter drilled anchor hole. The embedment depth varied between 8 and 12 times d_h depending on the location of internal steel reinforcement in the footing. In all but one test, an anchor fan length of 559 mm was

(a) **(b)**

Fig. 24. Failure of CF Anchor in C3 a) C-3-A1-330b) C-3-A2-280.

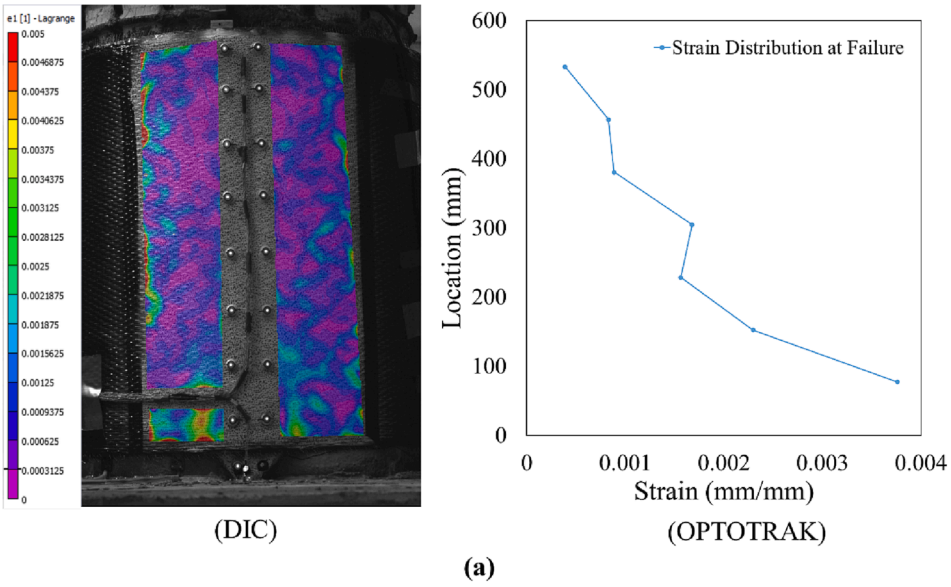

Fig. 25. Strain Distribution in Specimen C-3-A1-330 a) Vertical b) Hoop.

used. It may be possible to use a shorter anchor fan length when well-confined with a CFRP wrap, but that should be investigated as part of future research.

- Pull out of the anchor dowel was not observed in any test, and fiber rupture at the key portion of the anchor was achieved for well-confined anchor fans with an embedment depth of only $10d_h$. Hence, it is recommended that a $10d_h$ embedment depth is sufficient to achieve the full capacity of fanned anchor in direct tension. This is less than the recommended $13d_h$ embedment depth for straight anchors due to the reduced efficiency of fanned anchors and the lower demand on the anchor dowel.
- The proposed procedure to design the number of hoop fiber layers to confine the anchor fan and prevent a premature and undesirable debonding failure mode is effective and appears to be reasonably conservative when using a coefficient of friction along the debonding crack of 1.0, and a design hoop rupture strain of the CFRP wrap of 0.0058.
- For the well-confined anchor fan, the maximum measured vertical strain along the centerline of the anchor fan using DIC data (recorded from the exposed surface of the outermost layer of the CFRP wrap) was in the order of 0.005 at rupture failure of the key portion of the anchor. This is approximately 50% of the rupture strain recorded for the same anchor in the straight anchor test series. This is noteworthy as it is similar to the 55% efficiency recorded for the same anchor in the fanned anchor test series.
- Two of the anchors tested in this series were subject to a single cycle that would have induced a significant compression stress in the anchor prior to testing in tension. Unfortunately, the extent to which the compression stress affected the tensile capacity of the anchor was inconclusive. It is recommended that this be investigated further as part of future research. This is an important consideration for anchors subject to cyclic loading as in seismic retrofit applications.

CRediT authorship contribution statement

Emrah Tasdemir: . **Rudolf Seracino:** Conceptualization, Project administration, Supervision, Writing – review & editing. **Mervyn J. Kowalsky:** Conceptualization, Funding acquisition, Supervision, Writing – review & editing. **James Nau:** Conceptualization, Supervision, Writing – review & editing.

Declaration of Competing Interest

The authors declare that they have no known competing financial interests or personal relationships that could have appeared to influence the work reported in this paper.

Data availability

Data will be made available on request.

Acknowledgments

The authors would like to thank the Alaska Department of Transportation and Public Facilities [Federal #: 4000(142); IRIS #: Z839740000] for their support of this research program, and the Turkish Ministry of Education for supporting the graduate education of Emrah Tasdemir. The authors would like to thank Dr. Gregory Lucier, Jerry Atkinson and Johnathan McEntire at Constructed Facilities Laboratory (CFL) for their help during this research program. The authors would also like to thank Simpson Strong-Tie Company, Inc., for their support of this research study.

References

[1] L. Koutas, T.C. Triantafillou, Use of anchors in shear strengthening of reinforced concrete T-beams with FRP, J. Compos. Constr. 17 (1) (2013) 101–107, https://doi.org/10.1061/(ASCE)CC.1943-5614.0000316.
[2] N. Eshwar, T.J. Ibell, A. Nanni, Effectiveness of CFRP Strengthening on Curved Soffit RC Beams, Adv. Struct. Eng. 8 (1) (Jan. 2005) 55–68, https://doi.org/10.1260/1369433053749607.
[3] E. Akın, E. Canbay, B. Binici, G. Özcebe, Testing and analysis of infilled reinforced concrete frames strengthened with CFRP reinforcement, J. Reinf. Plast. Compos. 30 (19) (2011) 1605–1620, https://doi.org/10.1177/0731684411424631.
[4] D.T. Lau, J.E. Woods, A concentric tube anchor system for fiber-reinforced polymer retrofit of reinforced concrete structural walls under extreme loads, Int. J. Prot. Struct. 9 (1) (2018) 77–98, https://doi.org/10.1177/2041419617732353.
[5] H. El-Sokkary, K. Galal, I. Ghorbanirenani, P. Léger, R. Tremblay, Shake table tests on FRP-rehabilitated RC shear walls, J. Compos. Constr. 17 (1) (2013) 79–90, https://doi.org/10.1061/(ASCE)CC.1943-5614.0000312.
[6] I. Vrettos, E. Kefala, T.C. Triantafillou, Innovative flexural strengthening of reinforced concrete columns using carbon-fiber anchors, ACI Struct. J. 110 (1) (2013) 63–70, https://doi.org/10.14359/51684330.
[7] S.T. Rutledge, M.J. Kowalsky, R. Seracino, J.M. Nau, Repair of Reinforced Concrete Bridge Columns Containing Buckled and Fractured Reinforcement by Plastic Hinge Relocation, J. Bridge Eng. 19 (8) (Aug. 2014) A4013001, https://doi.org/10.1061/(ASCE)BE.1943-5592.0000492.
[8] E. del Rey Castillo, D. Dizhur, M. Griffith, J. Ingham, Strengthening RC structures using FRP spike anchors in combination with EBR systems, Compos. Struct. 209 (2019) 668–685.
[9] S.J. Kim, S.T. Smith, Pullout Strength Models for FRP Anchors in Uncracked Concrete, J. Compos. Constr. 14 (4) (Aug. 2010) 406–414, https://doi.org/10.1061/(ASCE)CC.1943-5614.0000097.
[10] G. Ozdemir, U. Akyuz, Tensile capacities of CFRP anchors, Adv. Earthq. Eng. Urban Risk Reduct. 66 (2006) 471–487, https://doi.org/10.1007/1-4020-4571-9 31.
[11] T. Ozbakkaloglu, M. Saatcioglu, Tensile Behavior of FRP Anchors in Concrete, J. Compos. Constr. 13 (2) (Apr. 2009) 82–92, https://doi.org/10.1061/(ASCE)1090-0268(2009)13:2(82).
[12] Kobayashi K, Fujil S, Yabe Y, Tsukagoshi H, Sugiyama T (2001) Advanced wrapping system with CF-anchor – stress transfer mechanism of CF-anchor. In: Proceedings of the Fifth International Conference on Fibre-Reinforced Plastics for Reinforced Concrete Structures (FRPRCS-5), 16–18 July, pp. 379–388. Cambridge, UK.
[13] E. del Rey Castillo, M. Griffith, J. Ingham, Straight FRP anchors exhibiting fiber rupture failure mode, Compos. Struct. 207 (2019) 612–624.
[14] R. Kalfat, R. Al-Mahaidi, S.T. Smith, Anchorage Devices Used to Improve the Performance of Reinforced Concrete Beams Retrofitted with FRP Composites: State-of-the-Art Review, J. Compos. Constr. 17 (1) (2013) 14–33, https://doi.org/10.1061/(ASCE)CC.1943-5614.0000276.
[15] ACI 440.2R (2017) Guide for the Design and Construction of Externally Bonded FRP Systems. American Concrete Institute (ACI) Committee 440, Farming Hills, MI, USA.
[16] S. Grelle, L. Sneed, An Evaluation of Anchorage Systems for Fiber-Reinforced Polymer (FRP) Laminates Bonded to Reinforced Concrete Elements, Struct. Congr. (2011) 1157–1168, https://doi.org/10.1061/41171(401)103.
[17] A.S.T.M. Standard, D7205 , d7205m–06,, Standard test method for tensile properties of fiber reinforced polymer matrix composite bars, ASTM International, West Conshohocken, Philadelphia, PA, USA, 2011.
[18] E.A. Ahmed, E.F. El-Salakawy, B. Benmokrane, Tensile Capacity of GFRP Postinstalled Adhesive Anchors in Concrete, J. Compos. Constr. 12 (6) (Dec. 2008) 596–607, https://doi.org/10.1061/(ASCE)1090-0268(2008)12:6(596).
[19] Z. Achillides, K. Pilakoutas, Bond Behavior of Fiber Reinforced Polymer Bars under Direct Pullout Conditions, J. Compos. Constr. 8 (2) (Apr. 2004) 173–181, https://doi.org/10.1061/(ASCE)1090-0268(2004)8:2(173).
[20] B. Benmokrane, H.M. Mohamed, A.H. Ali, Service-life-prediction and field application of glass fiber-reinforced polymer tubular and solid bolts based on laboratory physical and mechanical assessment, J. Compos. Mater. 52 (24) (Oct. 2018) 3309–3323, https://doi.org/10.1177/0021998318764806.
[21] L. Barcley, M. Kowalsky, Seismic Performance of Circular Concrete Columns Reinforced with High-Strength Steel, J. Struct. Eng. U. S. 146 (2) (2020) 1–11, https://doi.org/10.1061/(ASCE)ST.1943-541X.0002452.
[22] H. Rasheed, B. Decker, A. Esmaeily, R. Peterman, H. Melhem, The Influence of CFRP Anchorage on Achieving Sectional Flexural Capacity of Strengthened Concrete Beams, Fibers 3 (4) (2015) 539–559, https://doi.org/10.3390/fib3040539.
[23] K.A. Harries, S.A. Carey, Shape and 'gap' effects on the behavior of variably confined concrete, Cem. Concr. Res. 33 (6) (Jun. 2003) 881–890, https://doi.org/10.1016/S0008-8846(02)01085-2.